Quantum transport in graphene

L1 Disordered graphene (G)

graphene 101

QHE in G and quantum resistance standard

weak localisation regimes in graphene

L2 Ballistic electrons in graphene

L3 Moiré superlattice effects in G/hBN heterostructures

sp^2 hybridisation forms strong directed covalent bonds between carbons (at 120°) which determine the honeycomb lattice structure

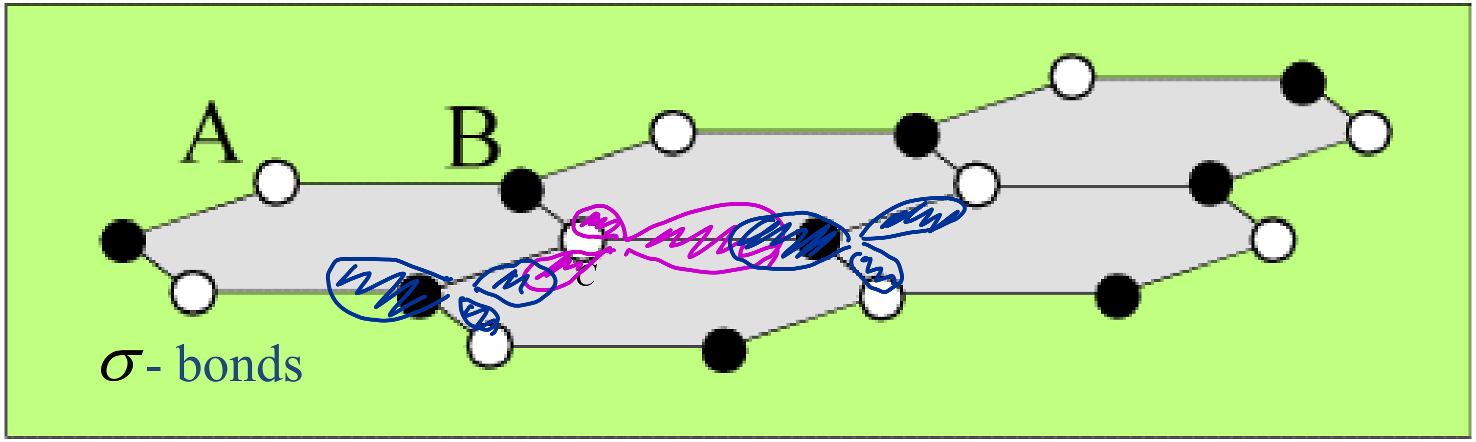

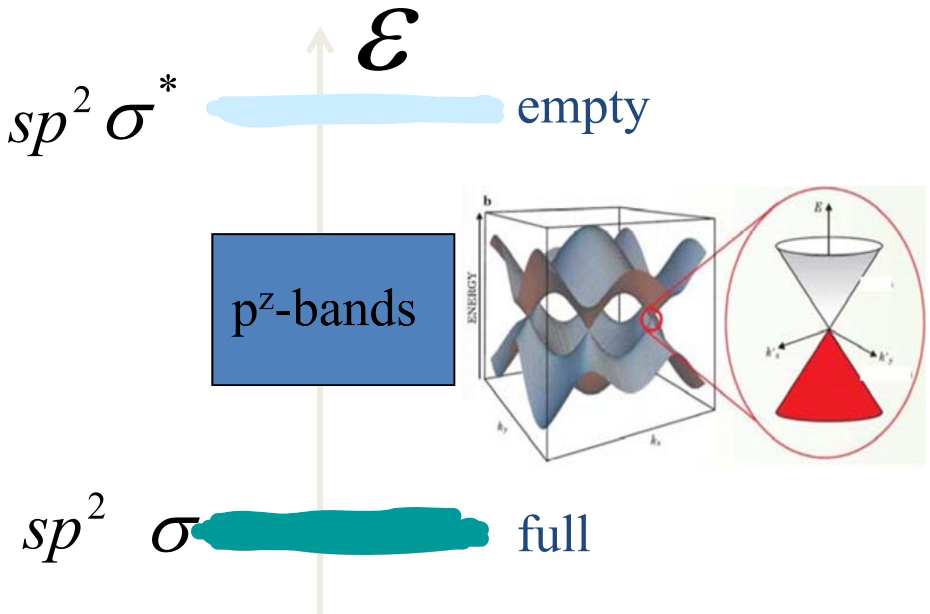

Graphenes

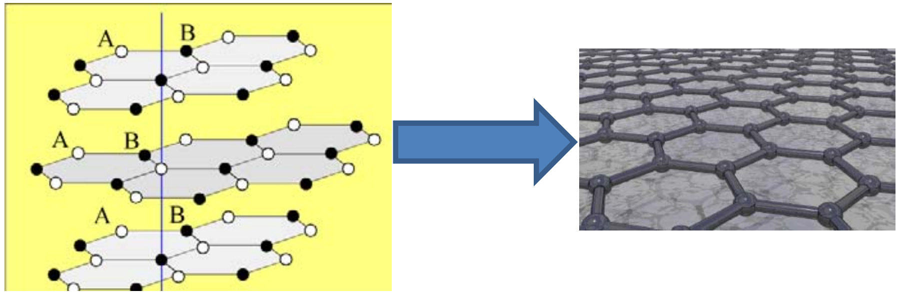

Exfoliated from bulk graphite onto a substrate, or hanged suspended (highest quality G/hBN in L2, L3)

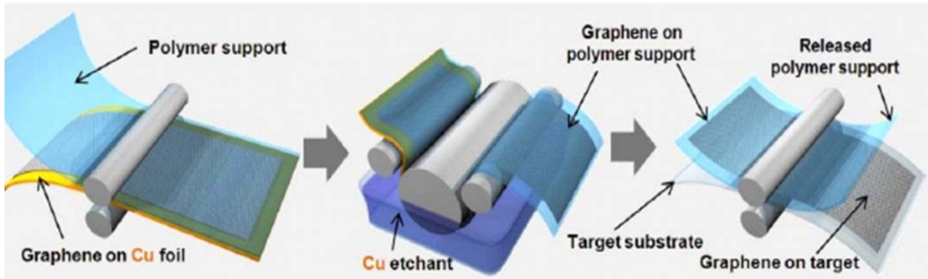

Grown using chemical vapor deposition (CVD) on metals (Cu, Ni), or insulators: polycrystalline and strained

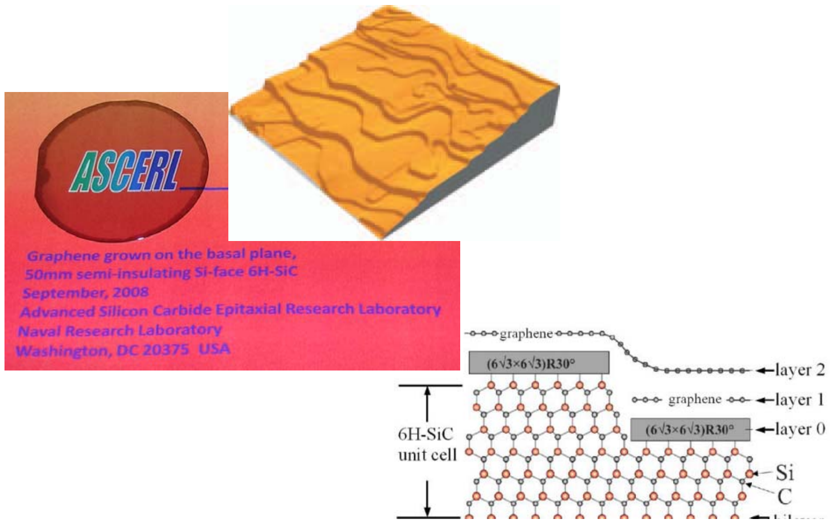

Epitaxial graphene sublimated on Si-terminated surface of SiC: wafer-scale single-crystalline carpet

Wallace, Phys. Rev. 71, 622 (1947)
Slonczewski, Weiss, Phys. Rev. 109, 272 (1958)

Transfer integral on a hexagonal lattice

$$\mathcal{H}_{AB} = \langle \Phi_A | H | \Phi_B \rangle$$

$$\mathcal{H}_{AB} = \frac{1}{N} \sum_{\mathbf{R}_A}^{N} \sum_{\mathbf{R}_B}^{N} e^{i\mathbf{k}.(\mathbf{R}_B - \mathbf{R}_A)} \underbrace{\langle \phi_A(\mathbf{r}-\mathbf{R}_A) | H | \phi_B(\mathbf{r}-\mathbf{R}_B) \rangle}_{\gamma_0}$$

sum over 3 nearest neighbour positions

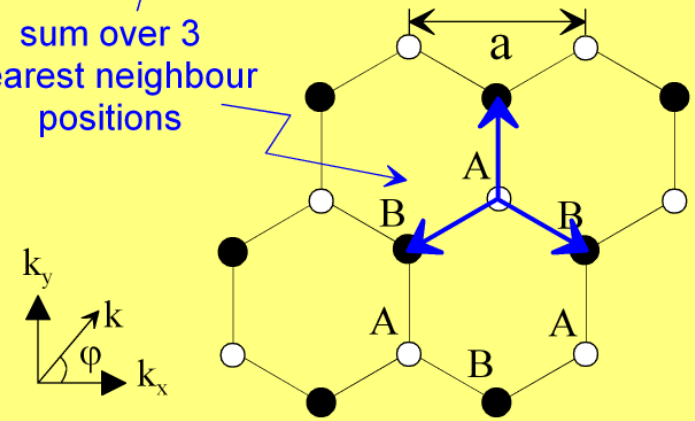

$$\mathcal{H}_{AB} = -\gamma_0 f(\mathbf{k}) \; ; \quad \mathcal{H}_{BA} = -\gamma_0 f^*(\mathbf{k})$$

$$f(\mathbf{k}) = e^{ik_y a/\sqrt{3}} + 2e^{-ik_y a/2\sqrt{3}} \cos(k_x a/2)$$

Tight binding model of a monolayer

Saito *et al*, "Physical Properties of Carbon Nanotubes" (Imperial College Press, London, 1998): Chapter 2.

Bloch function
$$\Phi_j(\mathbf{k}, \mathbf{r}) = \frac{1}{\sqrt{N}} \sum_{\mathbf{R}_j}^{N} e^{i\mathbf{k}.\mathbf{R}_j} \phi_j(\mathbf{r}-\mathbf{R}_j)$$

sum over N atomic positions

j^{th} atomic orbital: j = A or B

Eigenfunction
$$\Psi_j(\mathbf{k}, \mathbf{r}) = \sum_{i=1}^{2} C_{ji}(\mathbf{k}) \Phi_i(\mathbf{k}, \mathbf{r})$$

Transfer integral matrix $\mathcal{H}_{ij} = \langle \Phi_i | H | \Phi_j \rangle$

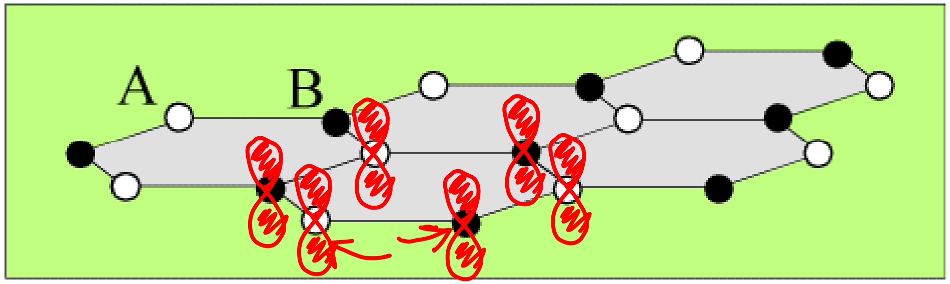

$$\gamma_0 \sim 3eV$$

Wallace, Phys. Rev. 71, 622 (1947)
Slonczewski, Weiss, Phys. Rev. 109, 272 (1958)

Transfer integral on a hexagonal lattice

$$\mathcal{H}_{AB} = \langle \Phi_A | H | \Phi_B \rangle$$

$$\mathcal{H}_{AB} = \frac{1}{N} \sum_{\mathbf{R}_A}^{N} \sum_{\mathbf{R}_B}^{N} e^{i\mathbf{k}.(\mathbf{R}_B - \mathbf{R}_A)} \underbrace{\langle \phi_A(\mathbf{r}-\mathbf{R}_A) | H | \phi_B(\mathbf{r}-\mathbf{R}_B) \rangle}_{\gamma_0}$$

sum over 3 nearest neighbour positions

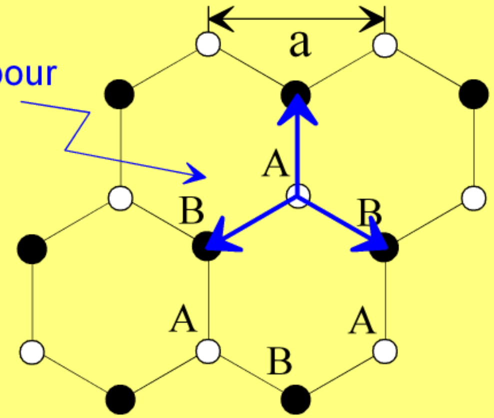

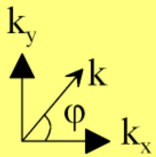

$$\mathcal{H}_{AB} = -\gamma_0 f(\mathbf{k}) \; ; \quad \mathcal{H}_{BA} = -\gamma_0 f^*(\mathbf{k})$$

$$f(\mathbf{k}) = e^{ik_y a/\sqrt{3}} + 2e^{-ik_y a/2\sqrt{3}} \cos(k_x a/2)$$

Tight binding model of a monolayer

Saito *et al*, "Physical Properties of Carbon Nanotubes" (Imperial College Press, London, 1998): Chapter 2.

Transfer integral matrix
$$\mathcal{H} = \begin{pmatrix} 0 & -\gamma_0 f(\mathbf{k}) \\ -\gamma_0 f^*(\mathbf{k}) & 0 \end{pmatrix}$$

Overlap integral matrix
$$S = \begin{pmatrix} 1 & s f(\mathbf{k}) \\ s f^*(\mathbf{k}) & 1 \end{pmatrix}$$

Eigenvalue equation $\quad \mathcal{H} C_j = \varepsilon_j S C_j$

$$\varepsilon = \frac{\pm \gamma_0 |f(\mathbf{k})|}{1 \mp s|f(\mathbf{k})|}$$

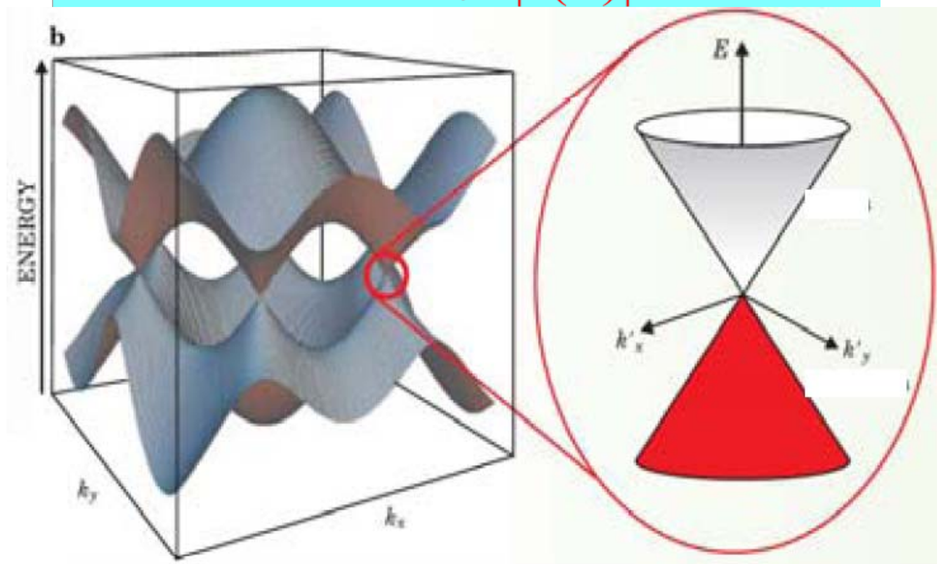

$$\sum_{\mathbf{R}_B}^{N} e^{i\mathbf{k}.(\mathbf{R}_B - \mathbf{R}_A)} \underbrace{\langle \phi_A(\mathbf{r}-\mathbf{R}_A)|H|\phi_B(\mathbf{r}-\mathbf{R}_B)\rangle}_{\gamma_0}$$

$$\Phi_j(\mathbf{k}, \mathbf{r}) = \frac{1}{\sqrt{N}} \sum_{\mathbf{R}_j}^{N} e^{i\mathbf{k}.\mathbf{R}_j}\, \phi_j(\mathbf{r}-\mathbf{R}_j)$$

First Brillouin zone

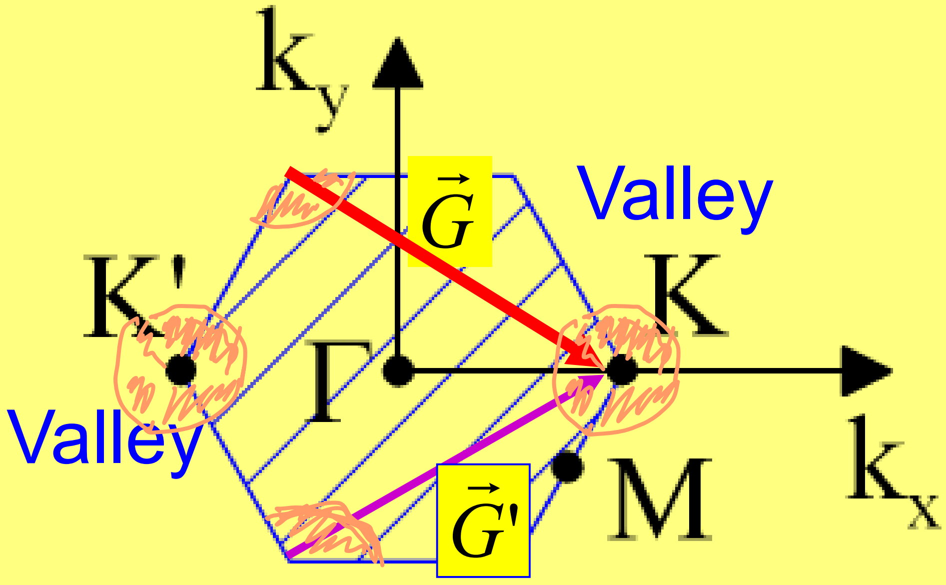

Two non-equivalent K-points

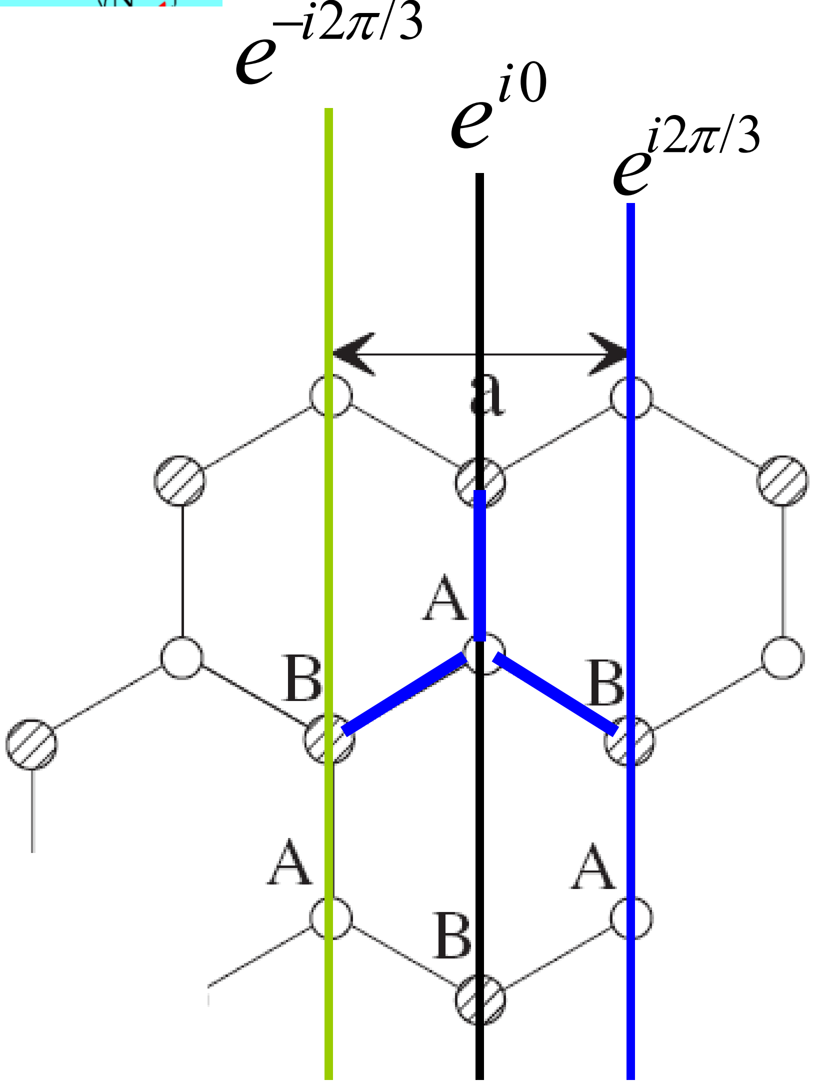

$$H_{AB,K} = -\gamma_0 \left[e^{-i\frac{2\pi}{3}} e^{-i\left(\frac{a}{2}p_x + \frac{a}{2\sqrt{3}}p_y\right)} + e^{i\frac{a}{\sqrt{3}}p_y} + e^{i\frac{2\pi}{3}} e^{i\left(\frac{a}{2}p_x - \frac{a}{2\sqrt{3}}p_y\right)} \right]$$

$$\approx -\frac{\sqrt{3}}{2}\gamma_0 a(p_x - ip_y)$$

$$H_{BA,K} \approx -\frac{\sqrt{3}}{2}\gamma_0 a(p_x + ip_y)$$

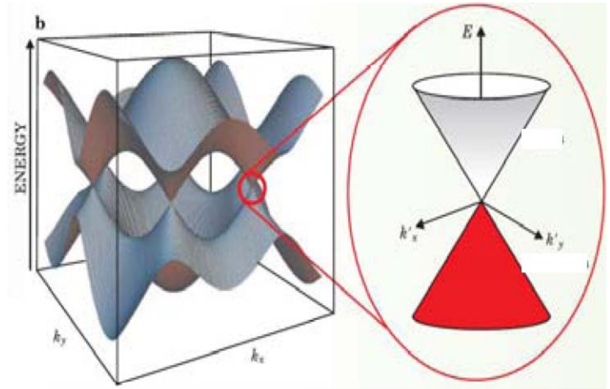

Bloch function amplitudes (e.g., in the valley K) on the AB sites (‘isospin’) mimic spin components of a massless relativistic particle.

$$\psi = \begin{pmatrix} \varphi_A \\ \varphi_B \end{pmatrix}$$

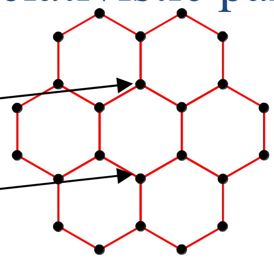

$$\hat{H} = -v \begin{pmatrix} 0 & p_x - ip_y \\ p_x + ip_y & 0 \end{pmatrix} = -v\vec{\sigma}\cdot\vec{p}$$

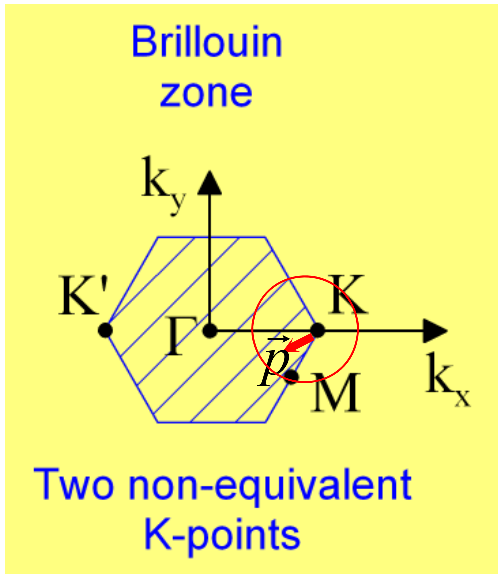

McClure, PR 104, 666 (1956)

$$v = \frac{\sqrt{3}}{2}\gamma_0 a \sim 10^8 \, \frac{cm}{\text{sec}}$$

$$\boxed{H = v\vec{\sigma}\cdot\vec{p}}$$

$$\vec{p} = (p\cos\vartheta, p\sin\vartheta)$$

Bloch function amplitudes on the A/B sites

$$\psi_K = \begin{pmatrix}\varphi_A \\ \varphi_B\end{pmatrix}$$

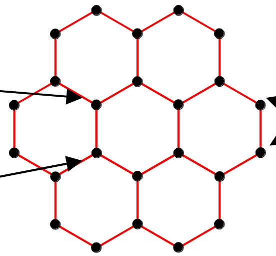

$$\begin{pmatrix}\varphi_B \\ -\varphi_A\end{pmatrix} = \psi_{K'}$$

Wave function.
sublattice composition
is linked to the axis
determined by the
electron momentum.

$$\varepsilon_c = vp$$

$$\psi_{\vec{p}} = \frac{1}{\sqrt{2}}\begin{pmatrix}1 \\ \pm e^{-i\vartheta}\end{pmatrix}$$

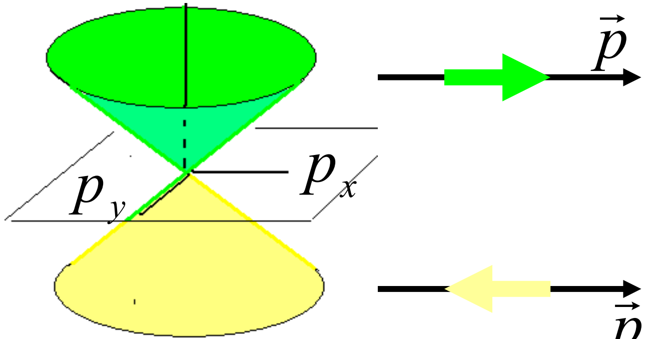

$$\varepsilon_v = -vp$$

for conduction band
electrons,

$$\vec{\sigma}\cdot\vec{n} = 1$$

$$\vec{\sigma}\cdot\vec{n} = -1$$

valence band (‘holes’)

Electronic states in graphene photographed using ARPES

high-energy photon
$\hbar\omega \sim 100 eV$

Simultaneous detection of the energy, E and propagation angle θ of photo-electrons enables one

$$p_{\|} = \sqrt{2mE}\cos\theta$$

$$\hbar\omega + \varepsilon(p_{\|}) - A = E$$

work function

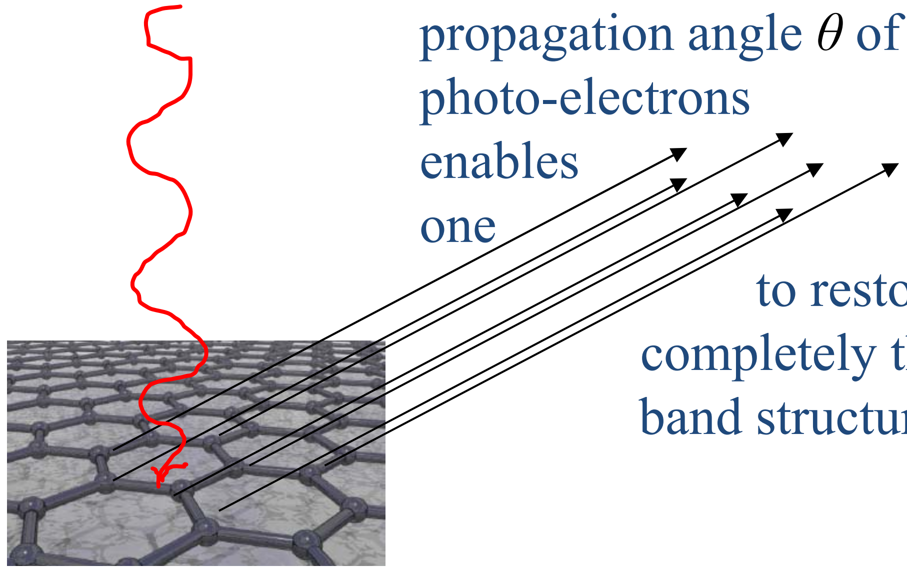

to restore completely the band structure.

Angle-resolved photo-emission spectroscopy (ARPES) of heavily doped graphene synthesized on silicon carbide

A. Bostwick *et al* – Nature Physics 3, 36 (2007)

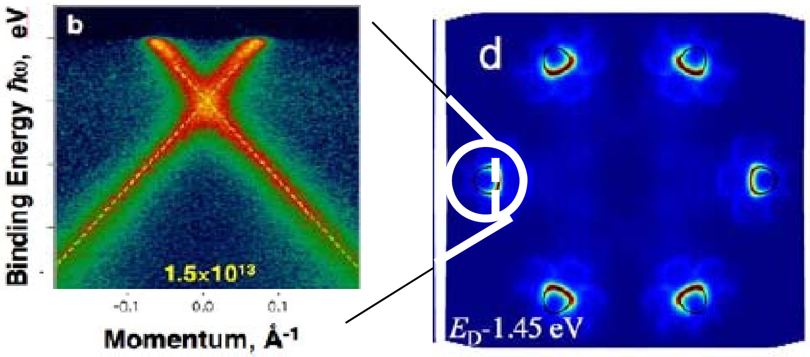

Electronic states in graphene photographed using ARPES

$$\psi = \begin{pmatrix} \varphi_A \\ \varphi_B \end{pmatrix}$$

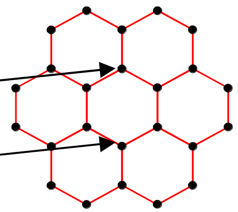

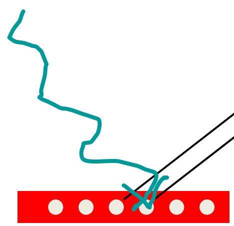

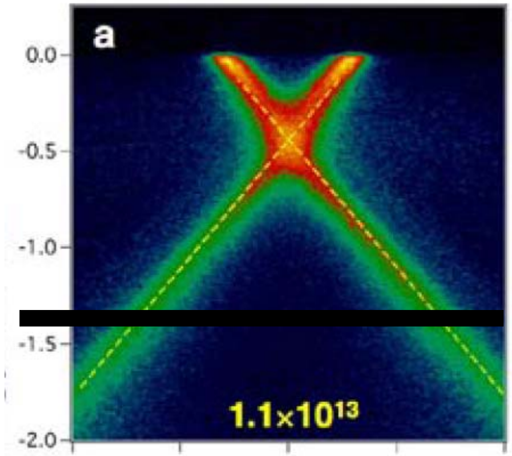

$$\varepsilon = -vp$$

$$I_{ARPES} \sim \left| \varphi_A + \varphi_B \right|^2$$

$$\sim \sin^2 \left(\frac{\vec{k} \cdot \vec{R}_{BA}}{2} + \frac{\vartheta}{2} \right)$$

$$\vec{k}_{\parallel} = \vec{G} \pm \vec{K} + \vec{p}$$

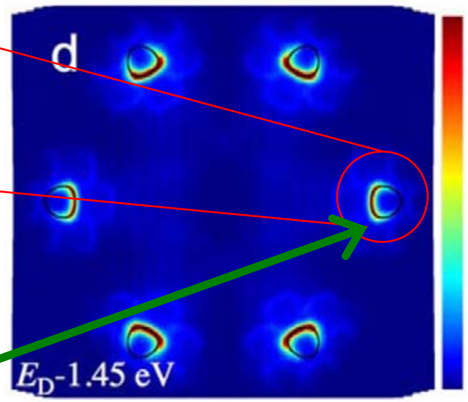

Mucha-Kruczynski, Tsyplyatyev, Grishin, McCann, Fal'ko, Boswick, Rotenberg - PRB 77, 195403 (2008)

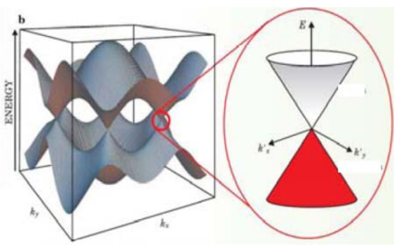

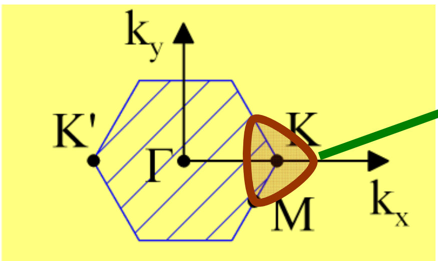

ARPES of heavily doped graphene synthesized on silicon carbide

Bostwick *et al* - Nature Physics 3, 36 (2007)

$$\varepsilon = vp$$

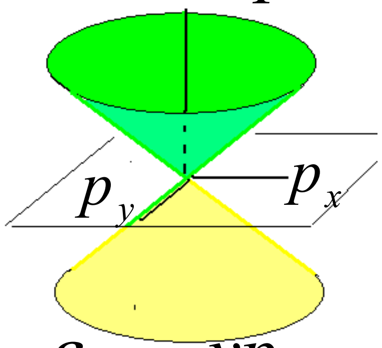

$$\varepsilon = -vp$$

$$\boxed{H = v\begin{pmatrix} 0 & \pi^{+} \\ \pi & 0 \end{pmatrix} = v\vec{\sigma}\cdot\vec{p}}$$

$$\vec{p} = (p\cos\vartheta, p\sin\vartheta)$$

$$\pi = p_x + ip_y = pe^{i\vartheta}$$

$$\pi^{+} = p_x - ip_y = pe^{-i\vartheta}$$

sublattice ‘isospin’ $\vec{\sigma}$ is linked to the direction of the electron momentum $\vec{p}$

conduction band

$$\vec{\sigma}\cdot\vec{n} = 1, \varepsilon = vp \qquad \vec{p}$$

$$\vec{\sigma}\cdot\vec{n} = -1, \varepsilon = -vp \qquad \vec{p}$$

valence band

$$\psi_{\vec{p}} = \frac{1}{\sqrt{2}}\begin{pmatrix} 1 \\ \pm e^{-i\vartheta} \end{pmatrix}$$

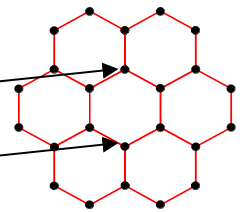

$$i\int_0^{2\pi} d\vartheta\, \psi^{+}\frac{d}{d\vartheta}\psi = \pi$$

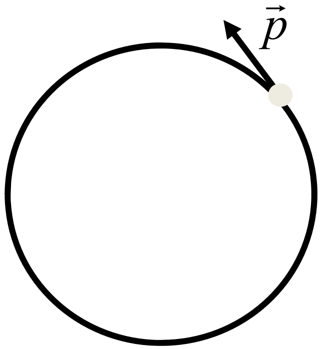

$$\psi \to e^{2\pi\frac{i}{2}\Sigma_3}\psi = e^{i\pi\Sigma_3}\psi = -\psi$$

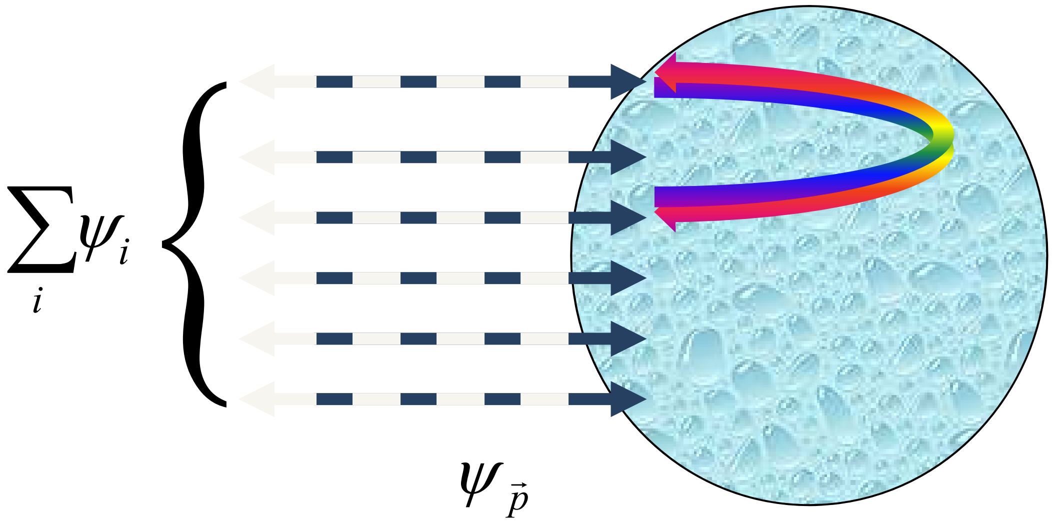

$$H = v\vec{\sigma}\cdot\vec{p} + \hat{1}\cdot U(x)$$

Simple A-B symmetric potential (smooth at the scale of lattice constant cannot scatter Berry phase π electrons in exactly backward direction.

$$\boxed{w_{\vec{p}\to-\vec{p}} = \left|\sum_i \psi_i\right|^2 = \left|\sum_{(a,b)}[\psi_{a\to b} + \psi_{b\to a}]\right|^2 = \left|\sum_{(a,b)} 0\right|^2 = 0}$$

$$\psi_{a\to b} = Ae^{i\frac{\pi}{2}\sigma_z}\psi_{\vec{p}}$$

$$\psi_{b\to a} = Ae^{i\frac{-\pi}{2}\sigma_z}\psi_{\vec{p}}$$

$$\Rightarrow \quad \psi_{a\to b} = e^{i\pi\sigma_z}\psi_{b\to a} = -\psi_{b\to a}$$

'Unstoppable' Berry phase π electrons

Graphene: gapless semiconductor

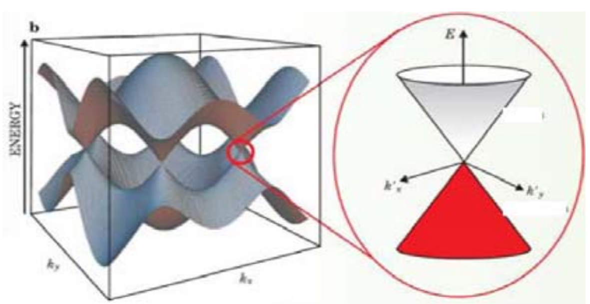

Wallace, Phys. Rev. 71, 622 (1947)

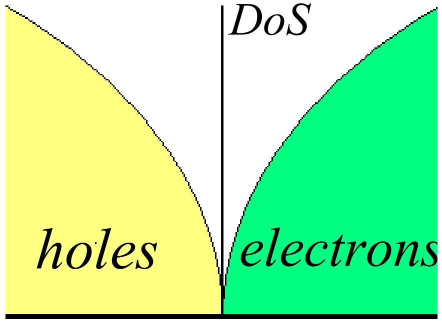

$$n_{carriers} \propto V_{gate}$$

Graphene-based field-effect transistor: GraFET (bipolar)

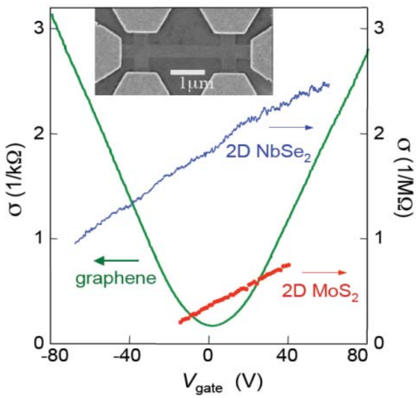

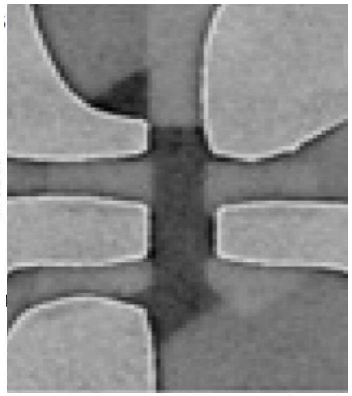

Geim and Novoselov, Nature Mat. 6, 183 (2007)

Quantum transport in graphene

L1 Disordered graphene (G)

graphene 101

QHE in G and quantum resistance standard

weak localisation regimes in graphene

L2 Ballistic electrons in graphene

L3 Moiré superlattice effects in G/hBN heterostructures

‘relativistic’ Landau levels

McClure, PR 104, 666 (1956)

$$\vec{p} = -i\hbar\vec{\nabla} - e\vec{A}$$

$$\pi = p_x + ip_y$$

$$\pi^+ = p_x - ip_y$$

$$\boxed{v\begin{pmatrix} 0 & \pi^+ \\ \pi & 0 \end{pmatrix}\begin{pmatrix} \psi_0 \\ 0 \end{pmatrix} = 0}$$

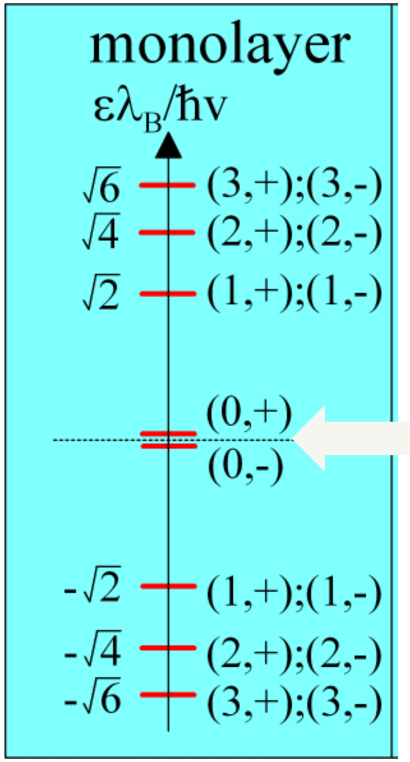

for valley K on A sublattice and valley K’ on B sublattice

$$\boxed{\varepsilon_n^{c/v} = \pm\sqrt{2n}\,\frac{\hbar v}{\lambda_B}}$$

$$v \sim 10^8\, cm/s$$

$$\lambda_B \equiv r_c^{(0)} = \sqrt{\frac{\hbar c}{eB}}$$

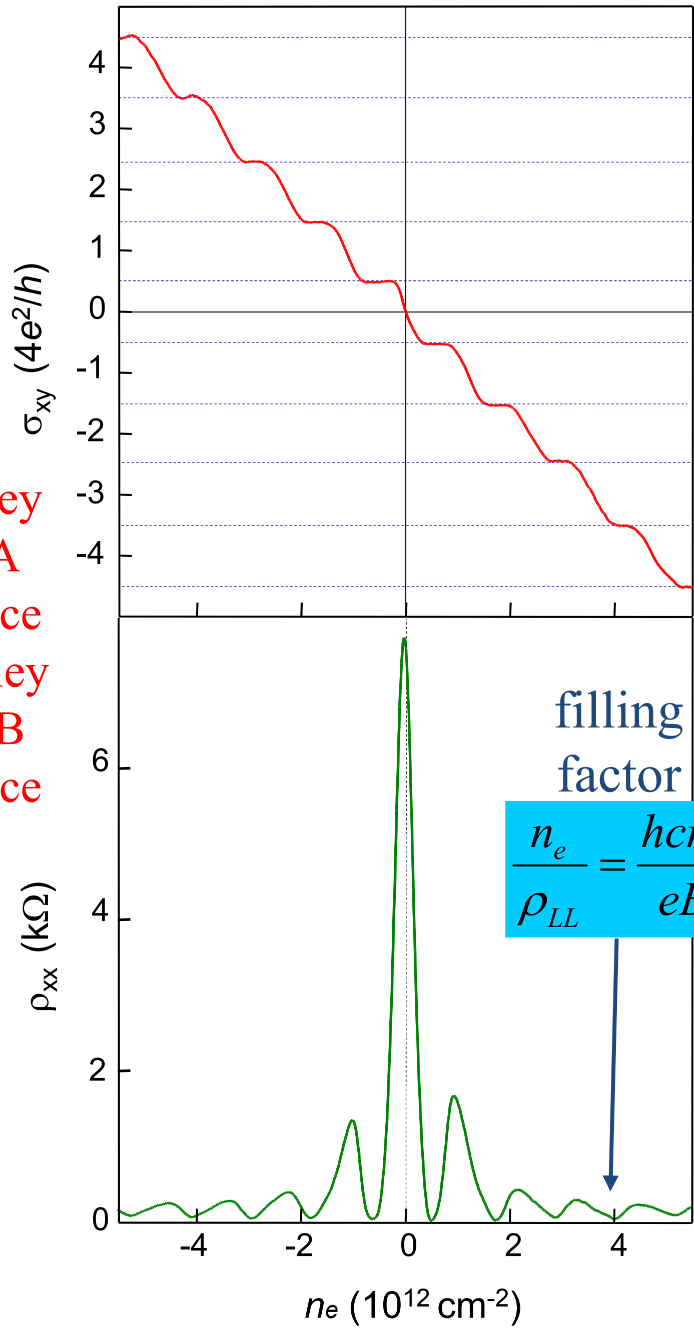

filling factor

$$\frac{n_e}{\rho_{LL}} = \frac{hcn_e}{eB}$$

$$H = v(\vec{p} - \tfrac{e}{c}\vec{A})\cdot\vec{\sigma}$$

the largest gaps in the LL spectrum

with 4-fold degenerate Landau level

McClure - Phys. Rev. 104, 666 (1956)

$$\Delta_{\nu=2} = \sqrt{2}\,\frac{v}{\lambda_B}$$

Novoselov *et al.*, Science 315, 1379 (2007).

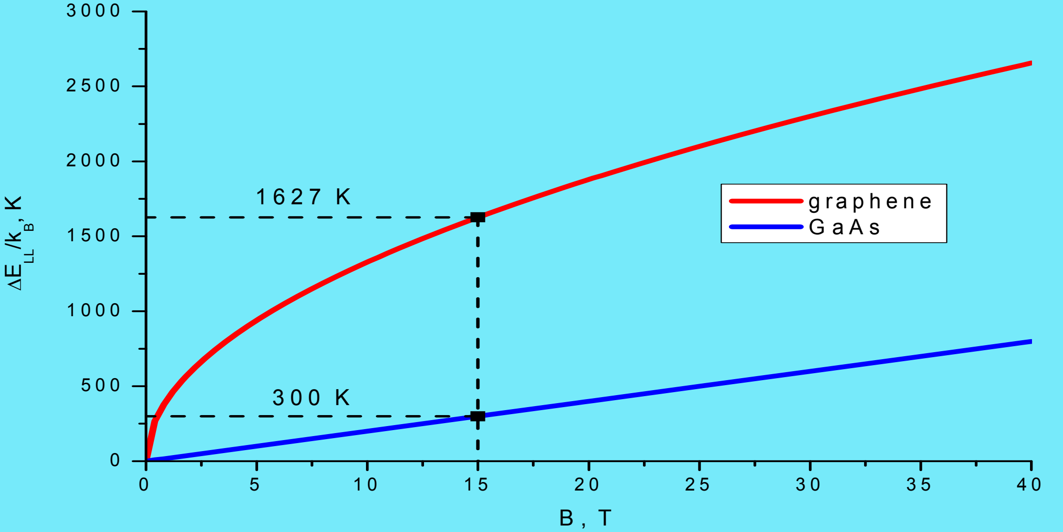

$$\nu = \pm 2$$

good for the quantum Hall effect in graphene with $R_{xy}=h/2e^2$

Epitaxial G/SiC (Si face)

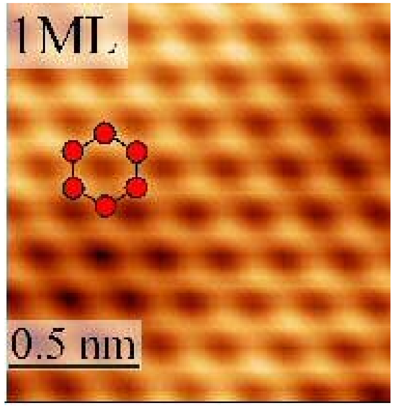

Lauffer, Emtsev, Graupner, Seyller **(Erlangen)**, Ley
PRB 77, 155426 (2008)

Gaskill et al, **(HRL Malibu)**
ECS Trans. 19, 117 (2009)

Dead layer with a large unit cell carries defects (missing C, Si substitutions of C, interstitial Si) in a large variety of positions, therefore, provides a broad band of surface donor/acceptor states which transfer charge to graphene

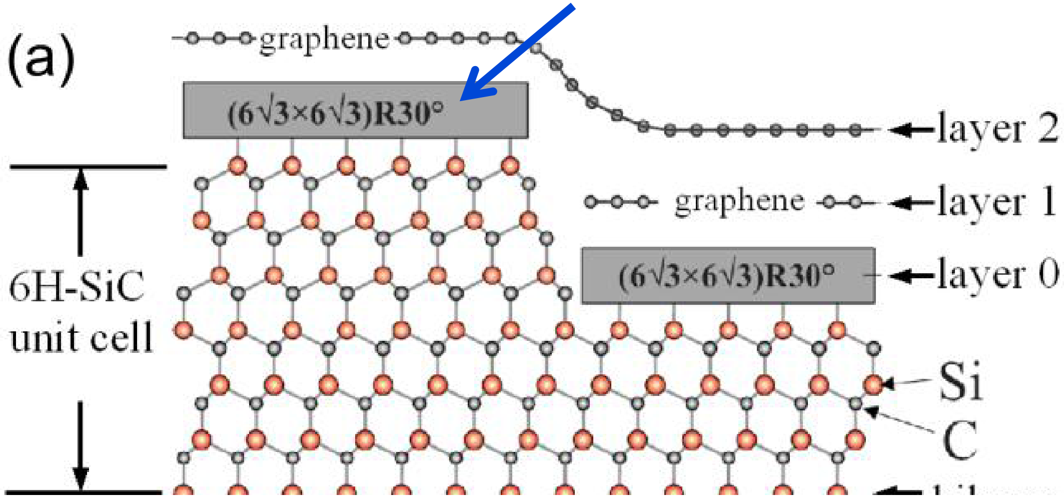

'Quantum capacitance' and charge transfer in G/SiC

classical capacitance

'quantum capacitance'

$$\gamma[A - 4\pi e^2 d(n+n_g) - \varepsilon_F(n)] + \rho l = n + n_g$$

surface donors DoS

bulk donors density

$$\tilde{A} = \varepsilon_F(n) + U + 4\pi e^2 d(n+n_g).$$

Schottky barrier

$$\varepsilon_F = \hbar v \sqrt{\pi n} \qquad U = 2\pi e^2 \rho l^2 / \chi$$

$$A = A_G - A_{surface\ donors}$$

$$\tilde{A} = A_G - A_{bulk\ donors}$$

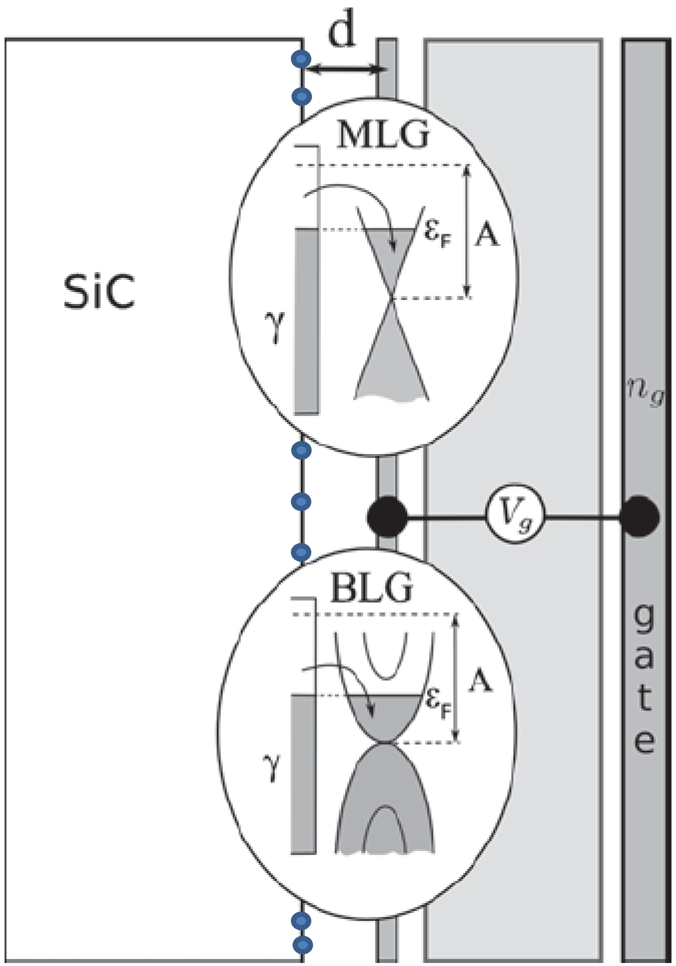

Kopylov, Tzalenchuk, Kubatkin, Fal'ko - Appl. Phys. Lett. 97, 112109 (2010)

G/SiC:
filling factor pinning

$$\gamma[A - 4\pi e^2 d(n+n_g) - \varepsilon_F(n)] + \rho l = n + n_g$$

$$\tilde{A} = \varepsilon_F(n) + U + 4\pi e^2 d(n+n_g).$$

$$\varepsilon_F = \sqrt{2N}\,\frac{\hbar v}{\lambda_B},\quad 4N-2 < \frac{nh}{eB} < 4N+2$$

$$\varepsilon_F = \hbar v\sqrt{\pi n}$$

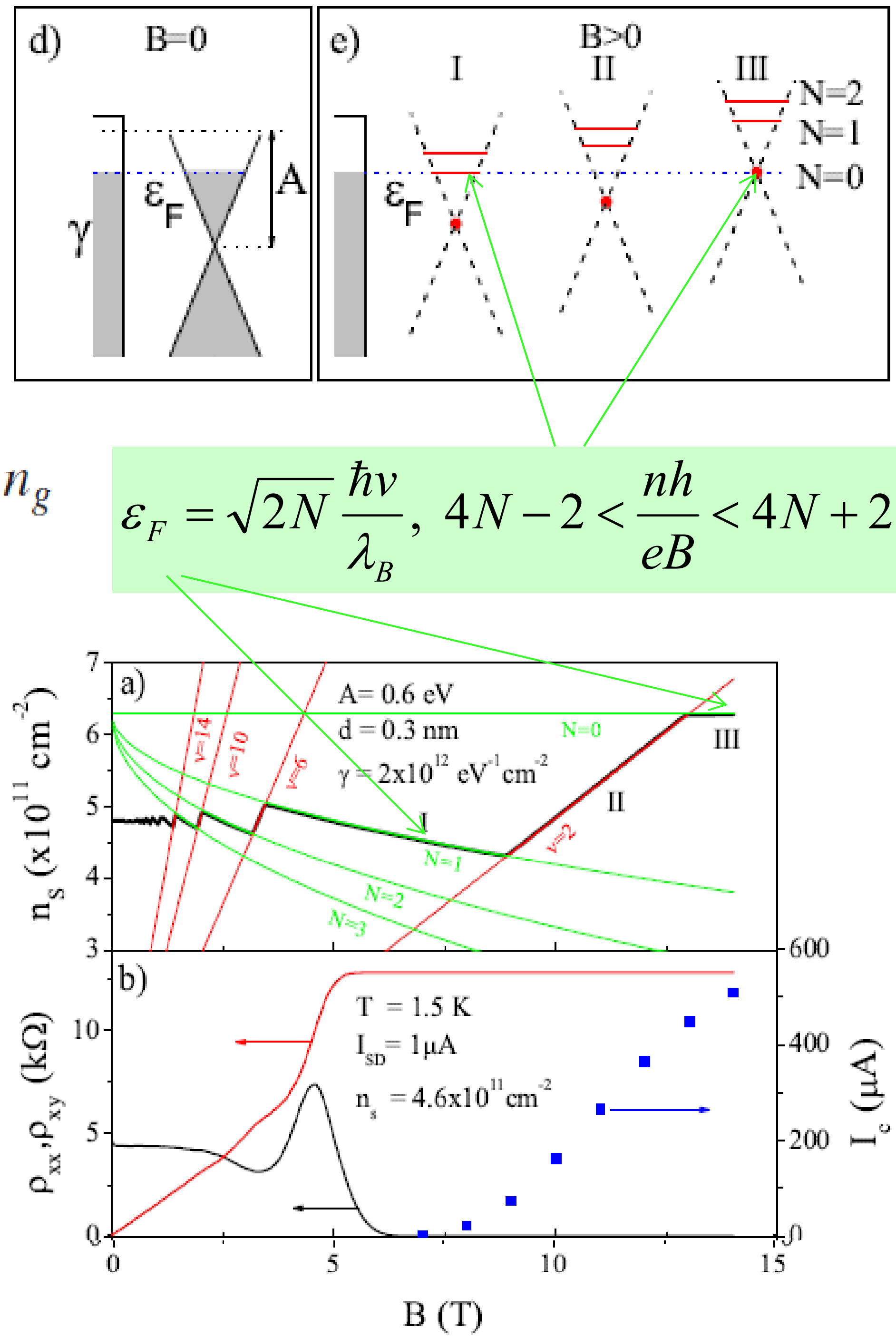

Due to the filling factor pinning, the largest QHE breakdown current is not at a nominal *B(ν=2)*, but appears at a higher field.

Janssen, Tzalenchuk, Yakimova, Kubatkin, Lara-Avila, Kopylov, Fal'ko - PRB 83, 233402 (2011)

Graphene-based resistance standard

Tzalenchuk, Lara-Avila, Kalaboukhov, Paolillo, Syväjärvi, Yakimova, Kazakova, Janssen, Fal'ko, Kubatkin
Nature Nanotechnology 5, 186 (2010)

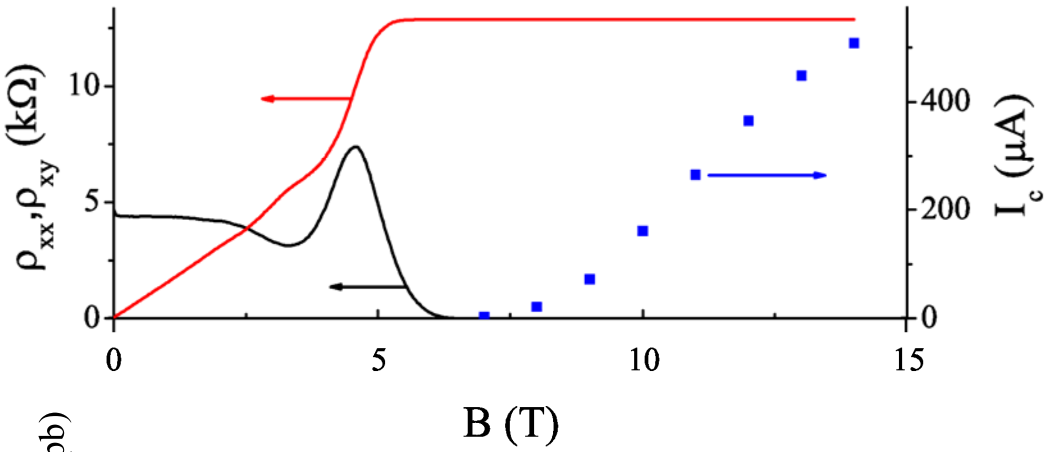

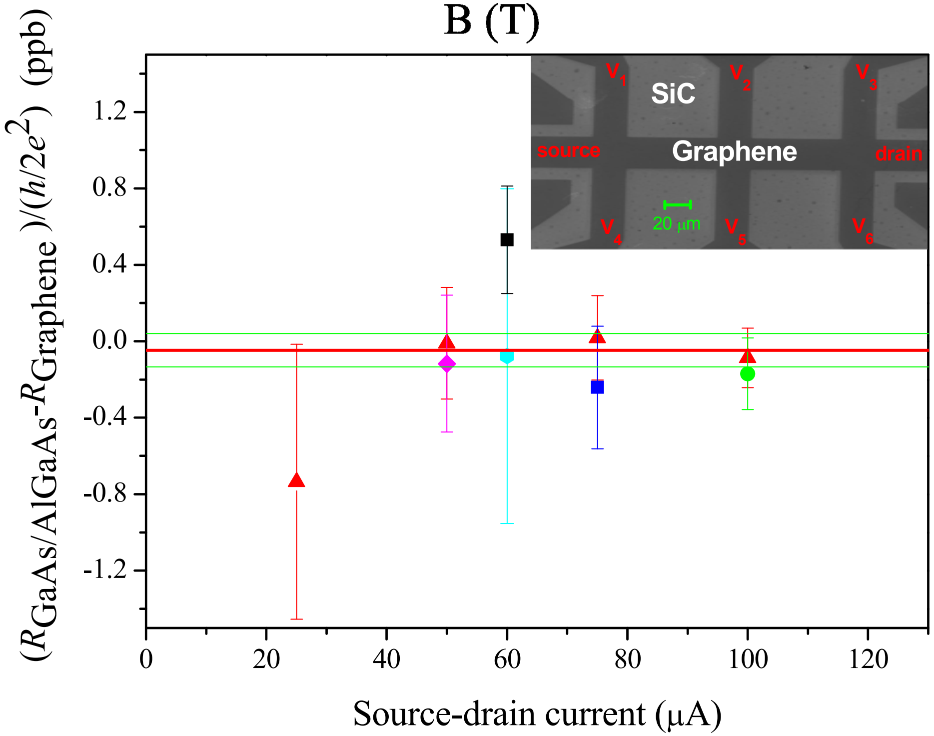

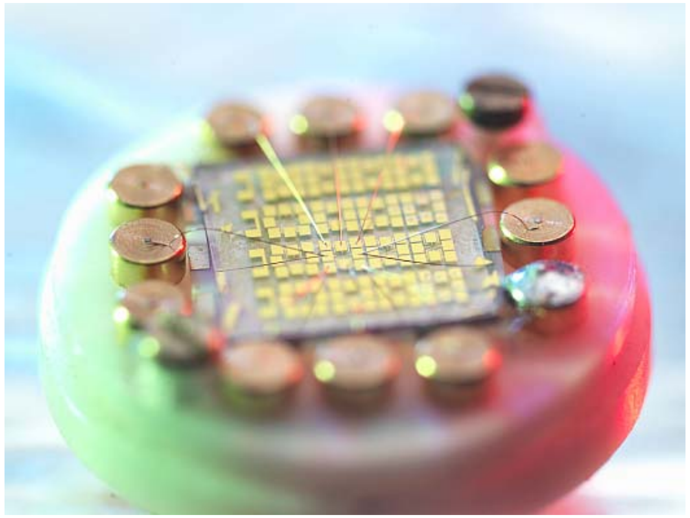

- 500 μA at 14 T and 300 mK
- 87 pp trillion (ppt)

Janssen, Tzalenchuk, Lara-Avila, Kubatkin, Fal'ko
Rep. Prog. Phys. 76, 104501 (2013)

Resistance metrology

XIX-XX centuries

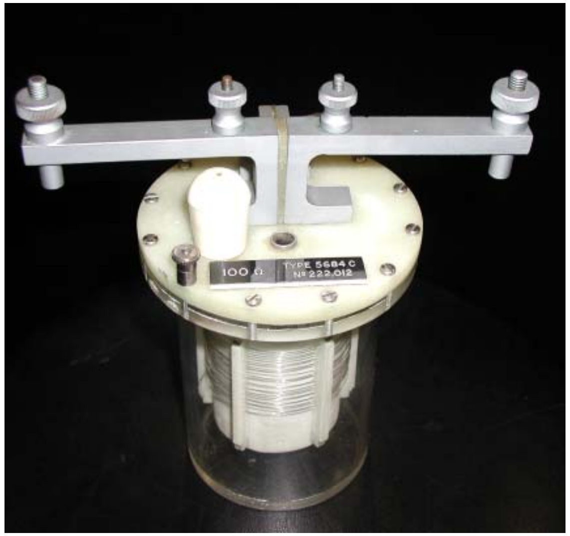

Wire resistor:
a unique artefact
which drifts in time

XXI century

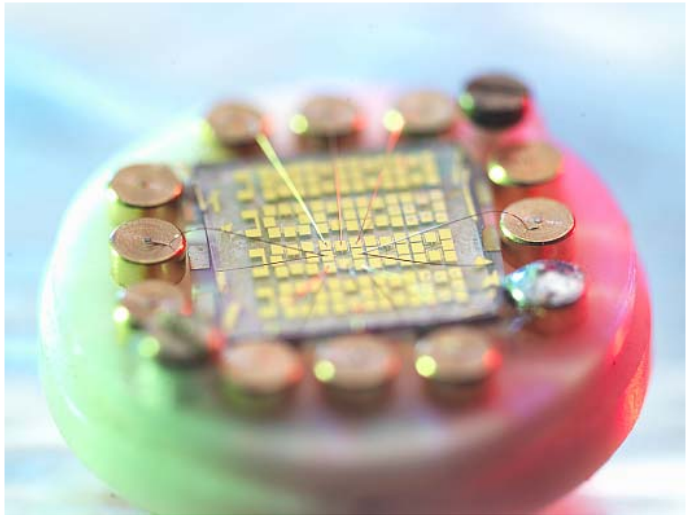

Quantum Hall effect:
universal and accurate

- **87 pp trillion (ppt)**

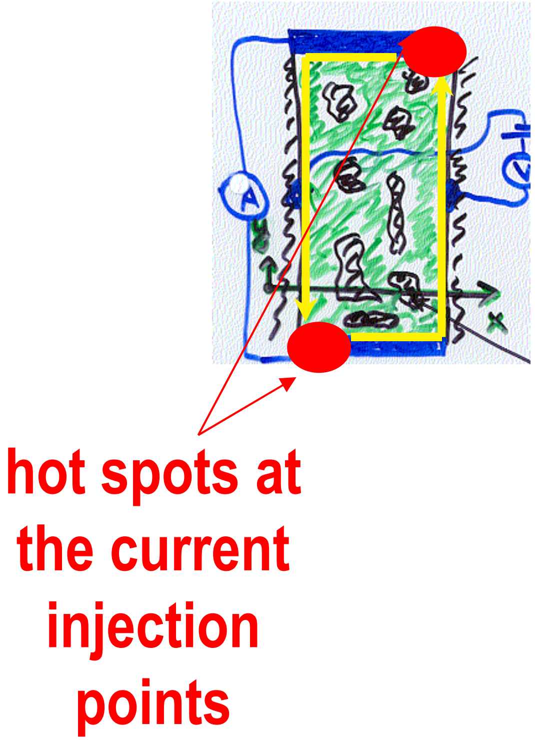

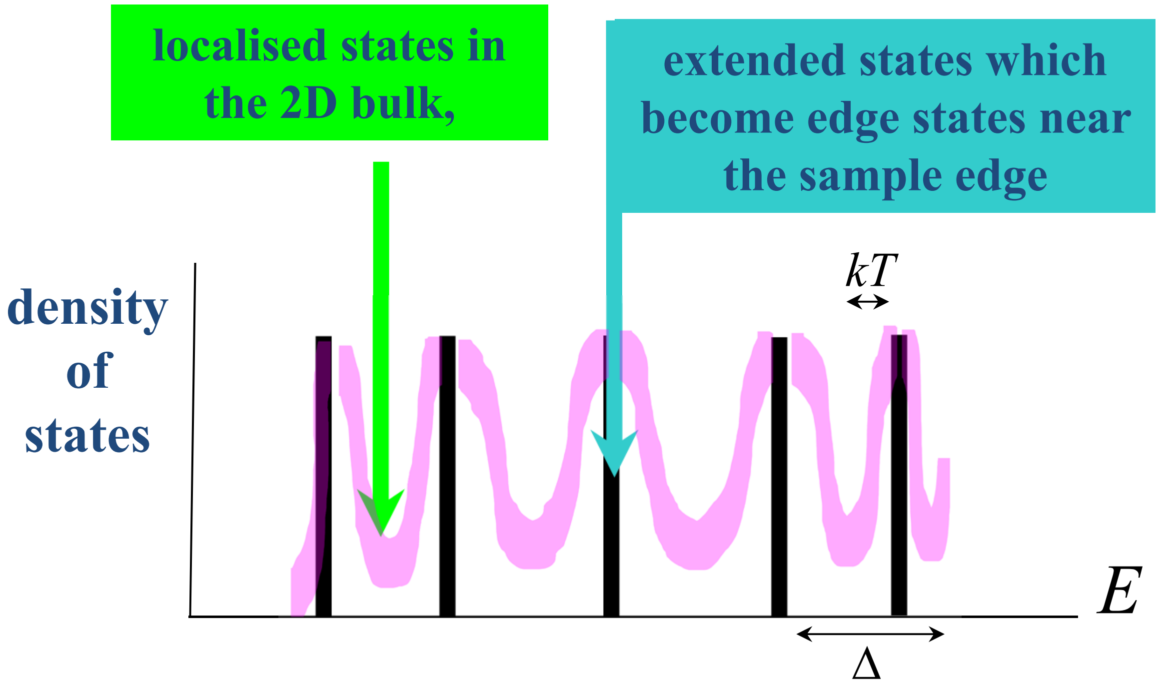

- Hall current is carried by electrons in the edge states extended along the edges and equipotential near metallic contacts, terminated at the current injection points
- Hot spots at the current injection contacts limit applicable current and therefore practical accuracy of quantisation

Edge states in graphene

$$\begin{cases} v\boldsymbol{\sigma}\cdot(-i\hbar\nabla + e\mathbf{A})\Psi = E\Psi\ ; \\ [1-(\boldsymbol{m}\cdot\boldsymbol{\tau})\otimes(\boldsymbol{n}\cdot\boldsymbol{\sigma})]\Psi|_{y=0} = 0; \\ \boldsymbol{n} = \hat{\mathbf{n}}_z\ \cos\phi + [\hat{\mathbf{n}}_z \times \mathbf{n}_\perp]\ \sin\phi. \end{cases}$$

B=0

$$P_{K\to -K} = \frac{(\tan\theta)^2}{(\cos\phi)^2 + (\tan\theta)^2}|\boldsymbol{m}\times\hat{\mathbf{n}}_z|^2.$$

$$E(p) = \xi\hbar v p \sin\phi$$

$$\Psi_\xi = \begin{bmatrix} \xi \\ \left(\tan\frac{\phi}{2}\right)^\xi \end{bmatrix} e^{-\xi p y \cos\phi + ipx}$$

Akhmerov & Beenakker, PRB 77, 085423 (2008)
Slizovskiy & Fal'ko, arXiv:1705.02866

QHE regime

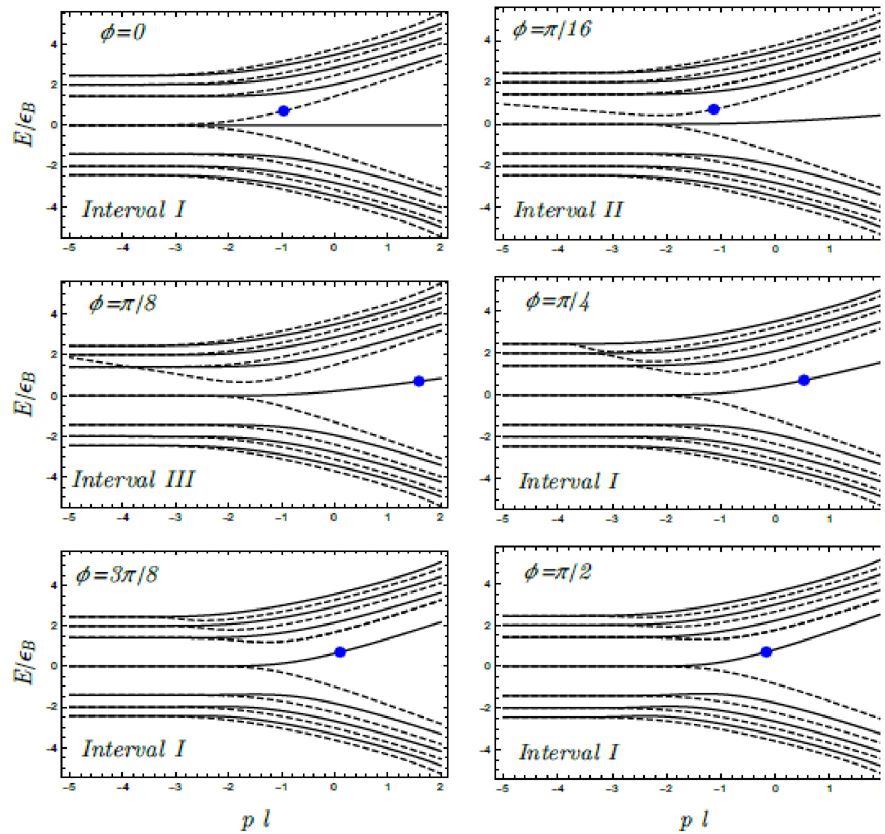

Current injection hot spot, chiral heat transport, and edge states cooling by phonons in G in vdW structures

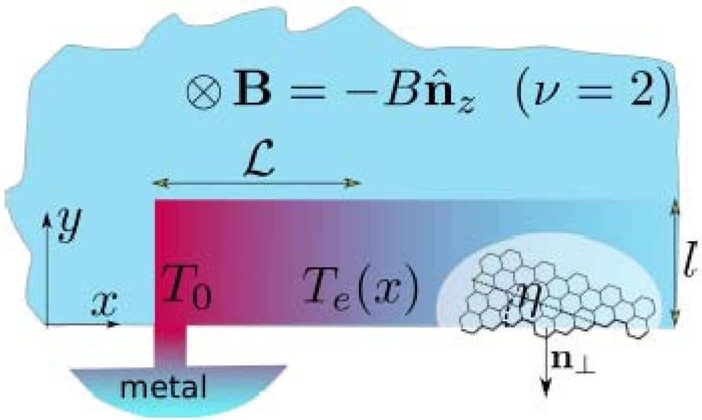

Nam, Hwang, Lee, Phys. Rev. Lett. 110, 226801 (2013)

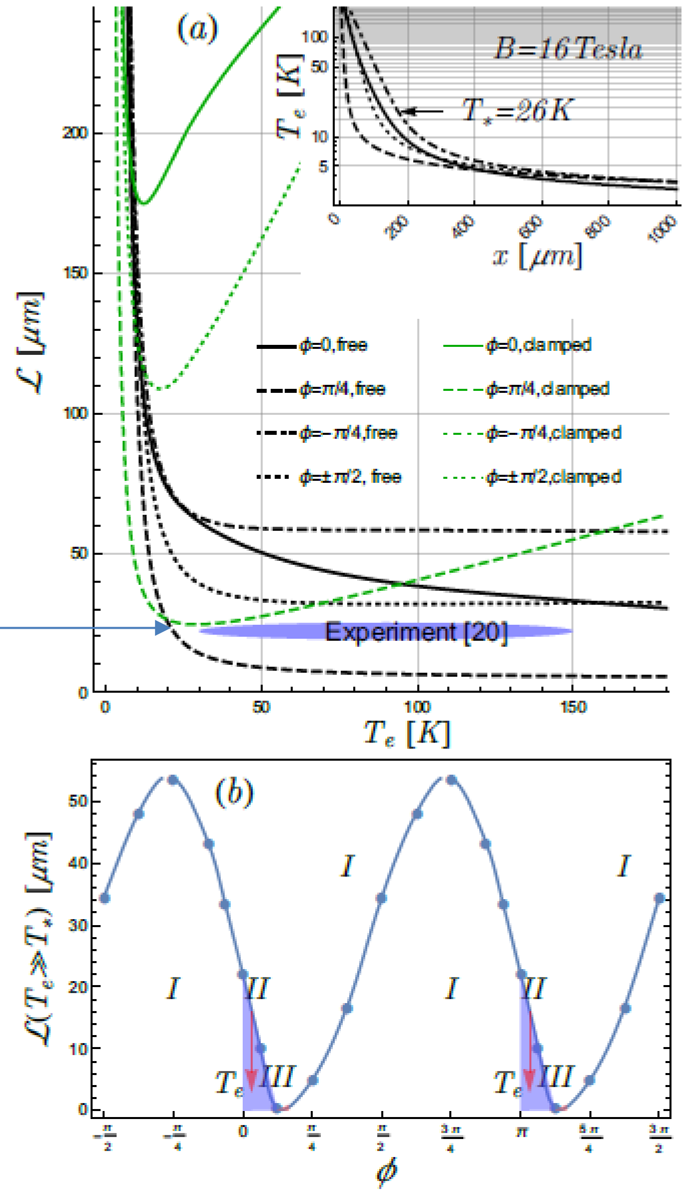

$$\mathcal{L}(T_e \gg T_*) \approx \frac{2\pi\hbar^2 \rho v_e^2 s}{g^2 r_0^2 e B}$$

Slizovskiy & Fal'ko, arXiv:1705.02866

Electrostatics of edge states in G/SiC

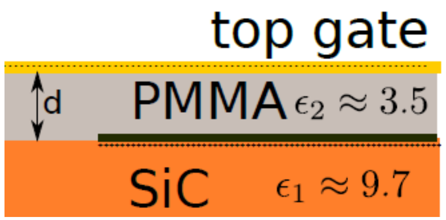

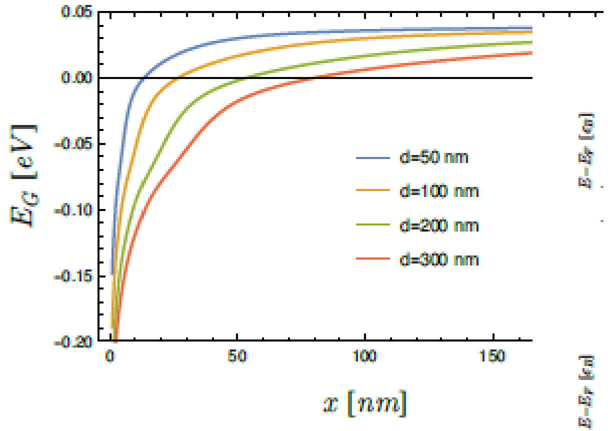

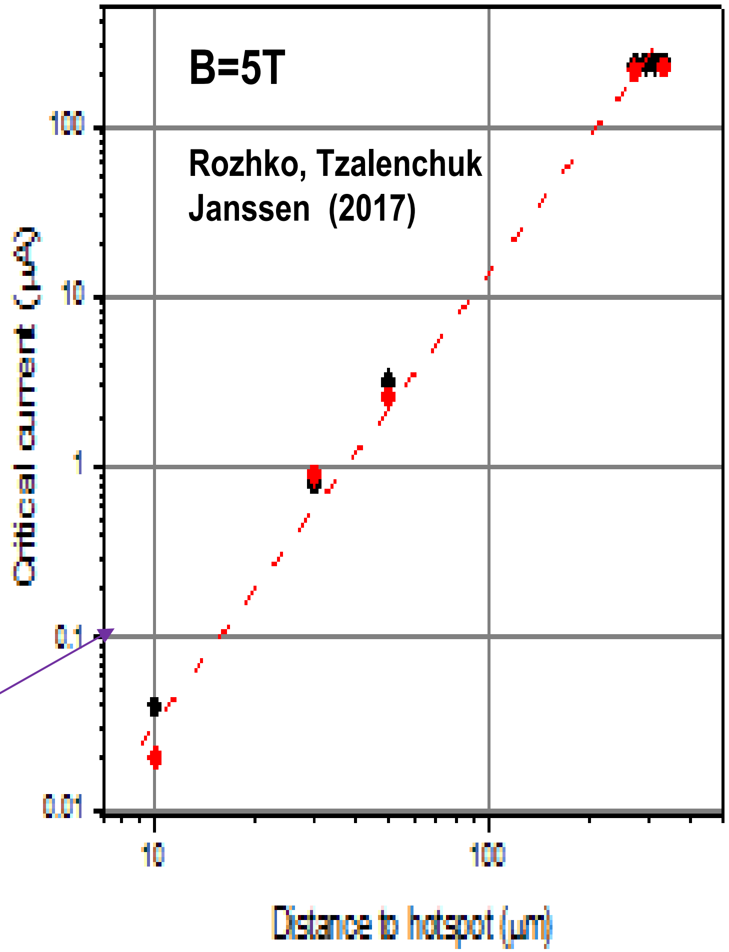

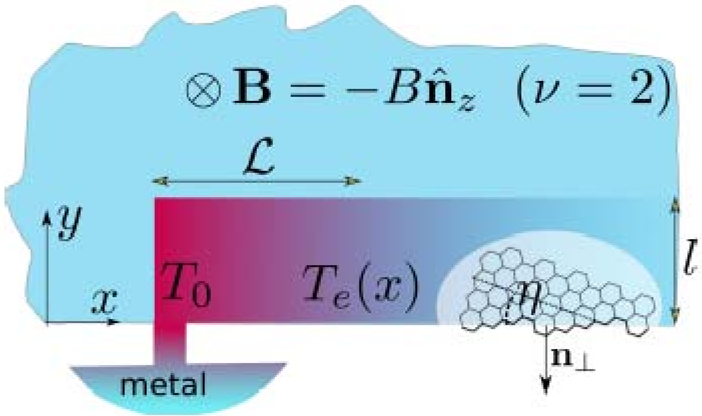

shorter T-decay length due to slower edge modes

$$\mathcal{L}(T_e \gg T_*) \approx \frac{2\pi\hbar^2 \rho v_e^2 s}{g^2 r_0^2 e B}$$

Slizovskiy & Fal'ko, 2017

Photochemical gating → Low-field QHE in G/SiC

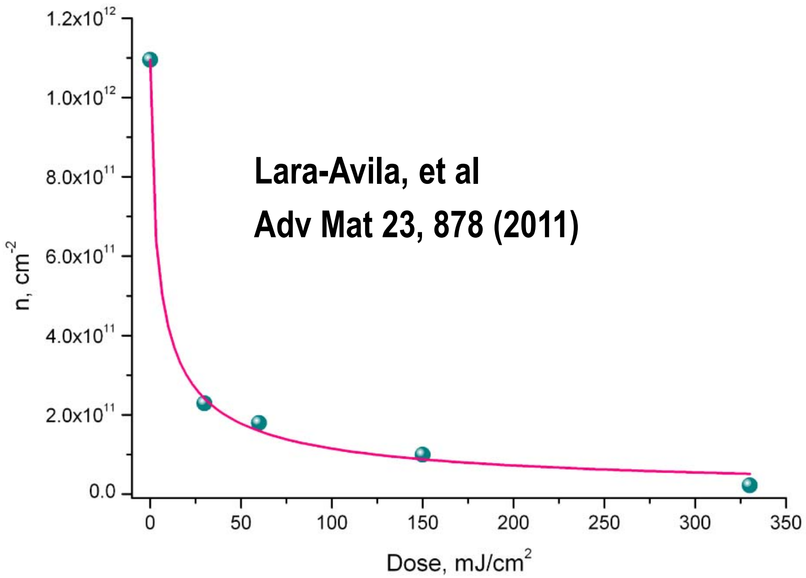

UV dose ↑
Carrier density ↓

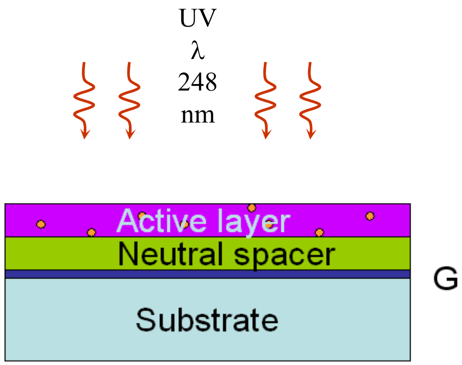

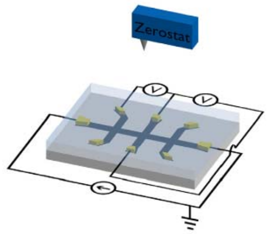

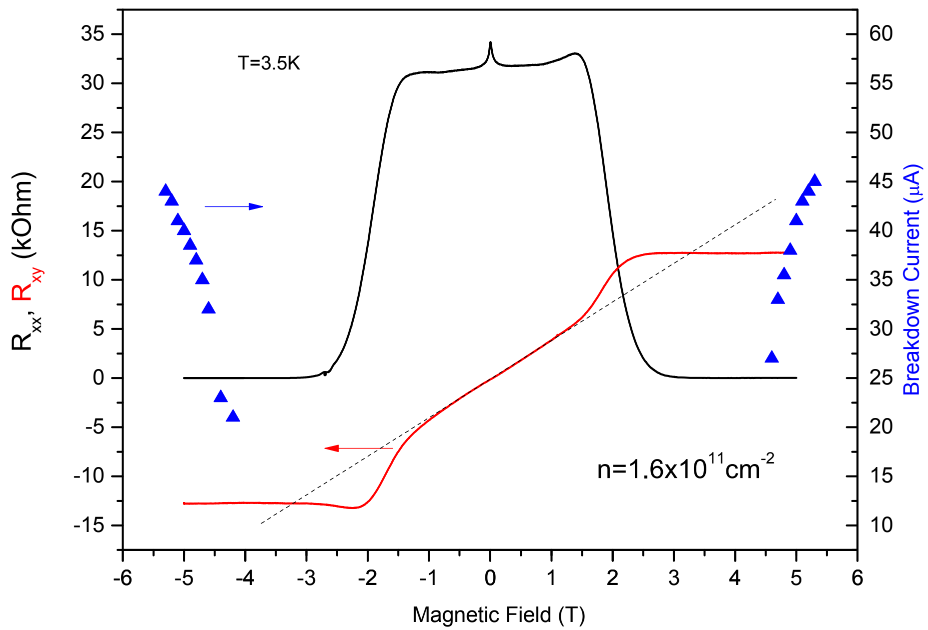

Commercial application of QHE: push-button QRS calibration tool

Oxford Instruments cryo-free system
NPL Cryogenic Current Comparator
optimal QRS device design (NGI)

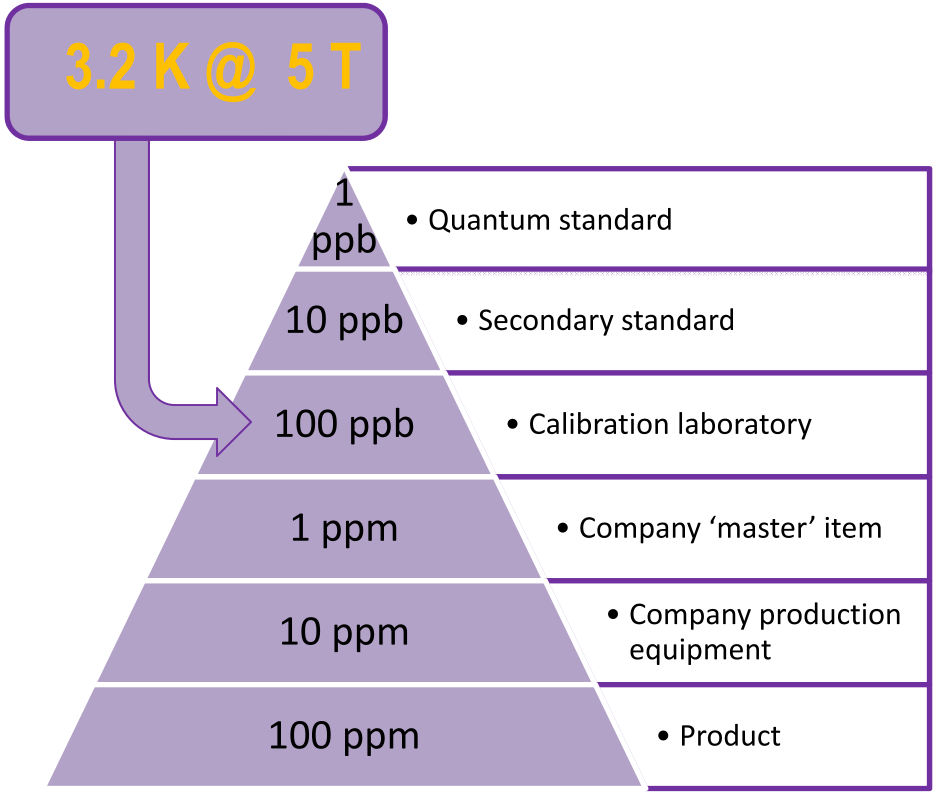

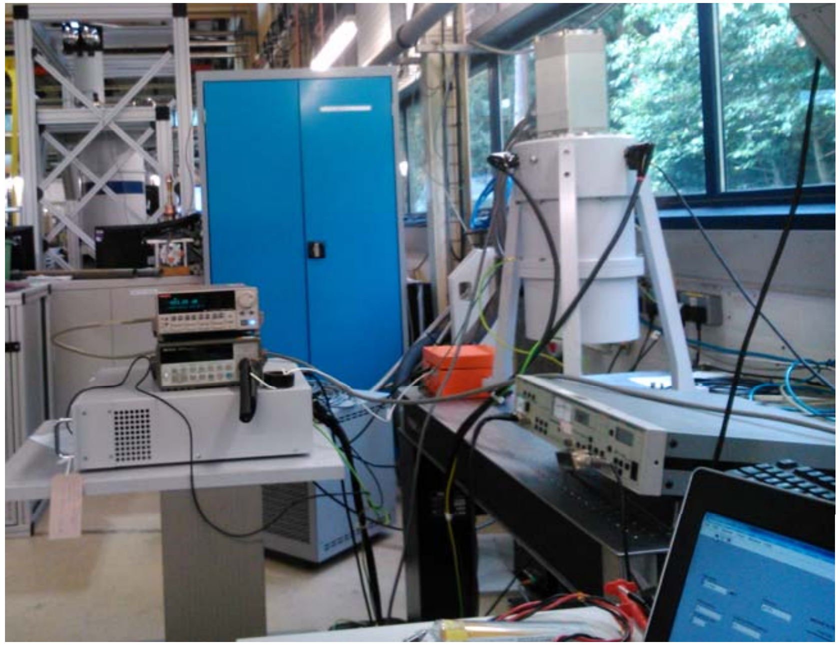

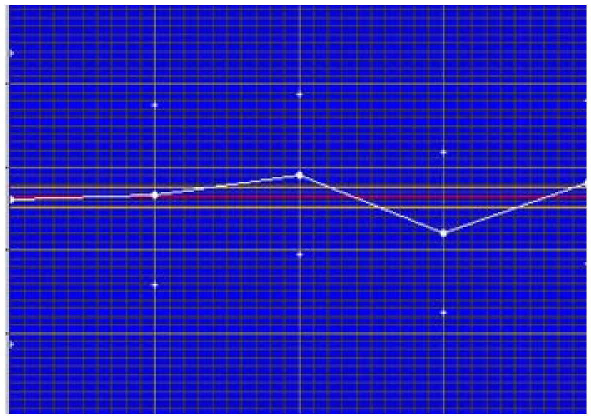

Quantum transport in graphene

L1 Disordered graphene (G)

graphene 101

QHE in G and quantum resistance standard

$\boxed{\text{weak localisation regimes in graphene}}$

L2 Ballistic electrons in graphene

L3 Moiré superlattice effects in G/hBN heterostructures

Interference correction to conductivity: Weak Localisation.

$$w \sim |A_\subset + A_\supset|^2 = |A_\subset|^2 + |A_\supset|^2 + [A_\subset^* A_\supset + A_\subset A_\supset^*]$$

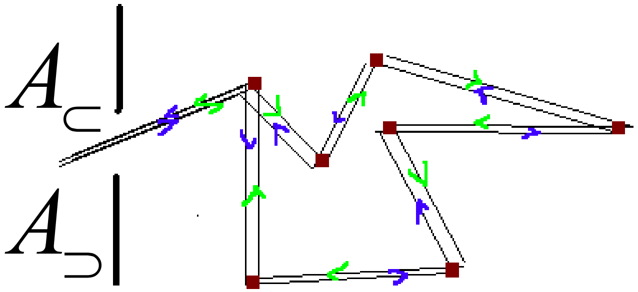

WL = enhanced backscattering for non-chiral electrons in time-reversal-symmetric systems

de-coherence suppresses interference contribution

$$\sigma = \sigma_{cl} - \frac{e^2}{2\pi h}\ln\left(\min[\tau_\varphi, \tau_B]/\tau\right)$$

time reversal symmetry breaking suppresses interference correction, leading to negative magnetoresistance

Interference correction to conductivity: Weak Localisation.

$$w \sim |A_{\subset} + A_{\supset}|^2 = |A_{\subset}|^2 + |A_{\supset}|^2 + [A_{\subset}^* A_{\supset} + A_{\subset} A_{\supset}^*]$$

$A_{\subset}$

$A_{\supset}$

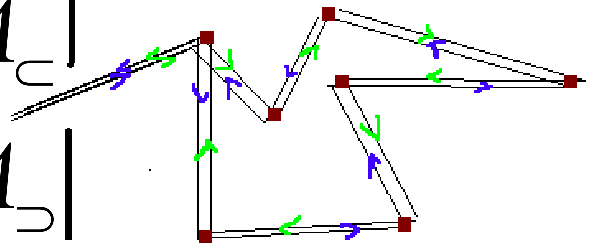

WL = enhanced backscattering **for non-chiral electrons in time-reversal-symmetric systems**

$$\sigma = \sigma_{cl} + \frac{e^2}{2\pi h} \ln\left(\min[\tau_{\varphi}, \tau_B]/\tau\right)$$

WAL = suppressed backscattering for Berry phase π electrons in MLG

chiral electrons $\psi_{out} = e^{-i\phi(\Sigma_z/2)} \psi_{in}$

$$A_{\subset} \sim e^{i\frac{\pi}{2}\Sigma_z} \psi_{\vec{p}}$$

$$A_{\supset} = e^{i\frac{-\pi}{2}\Sigma_z} \psi_{\vec{p}}$$

$$\Rightarrow \quad A_{\subset} A_{\supset}^* = e^{-i2\pi(\Sigma_z/2)} |A_{\subset}|^2 = -|A_{\subset}|^2 < 0$$

Strained graphene

$$\gamma_0 e^{-i\frac{2\pi}{3}} + \gamma_0 + \gamma_0 e^{i\frac{2\pi}{3}} = 0$$

$$\gamma_0' e^{-i\frac{2\pi}{3}} + \gamma_0'' + \gamma_0''' e^{i\frac{2\pi}{3}} = \alpha_x + i\alpha_y \neq 0$$

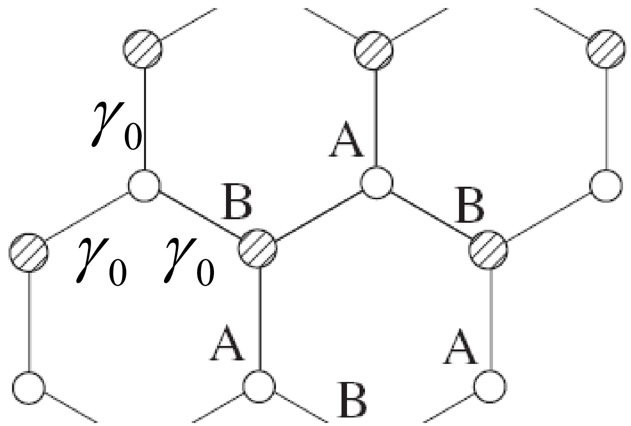

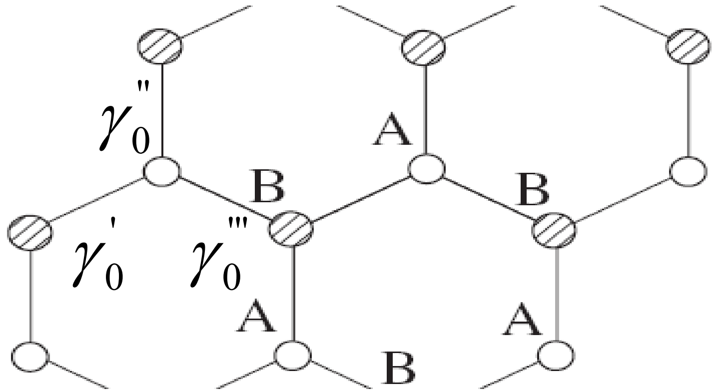

$$\hat{H} = v\vec{p}\cdot\vec{\Sigma} + \zeta\vec{\alpha}_{def}\cdot\vec{\Sigma} \equiv v[\vec{p} + \frac{\zeta}{v}\vec{\alpha}_{def}]\cdot\vec{\Sigma}$$

shift of the Dirac point in the momentum space, like some vector potential: opposite in K/K' valleys.

Iordanskii, Koshelev, JETP Lett 41, 574 (1985)
Ando - J. Phys. Soc. Jpn. 75, 124701 (2006)
Morpurgo, Guinea - PRL 97, 196804 (2006)

$$B_{eff} = \frac{\zeta}{v}[\nabla \times \vec{\alpha}_{def}(\vec{r})]_z$$

pseudo-magnetic-field, as if time inversion is lifted for electrons in each valley ($\zeta=\pm 1$ for K/K' valleys)

Strain-induced ‘100Tesla’ pseudo–magnetic fields in nanobubbles

Pseudo-Landau-levels due to pseudo-magnetic field in the nanobubbles

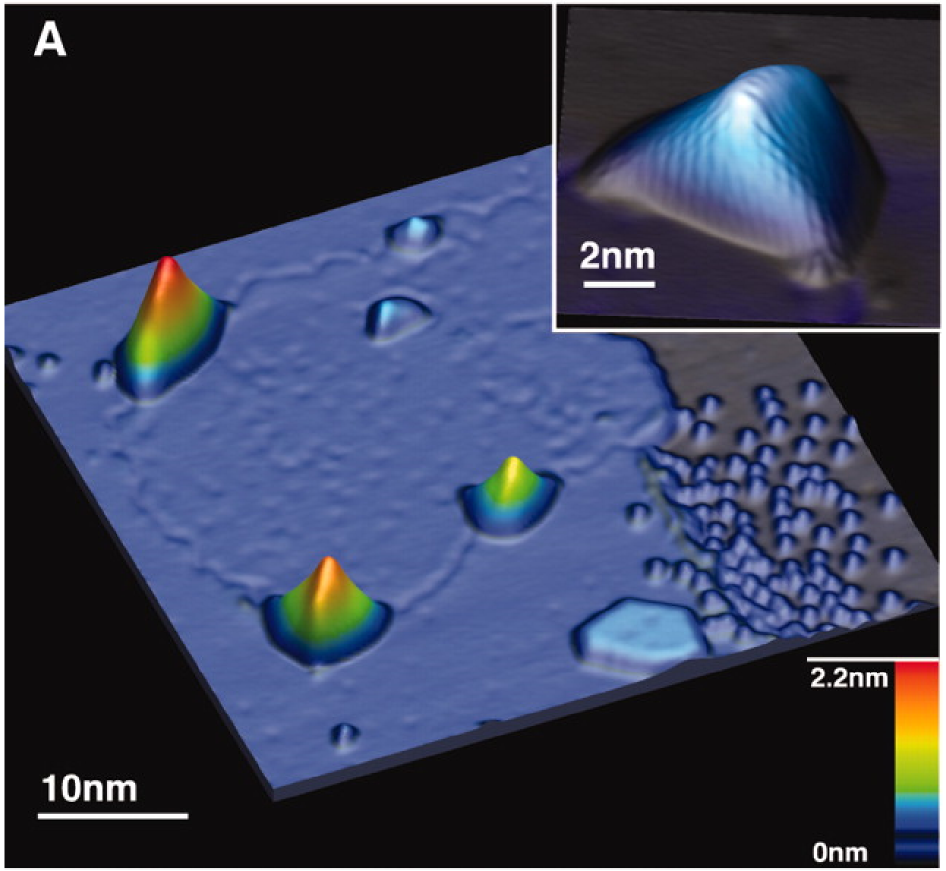

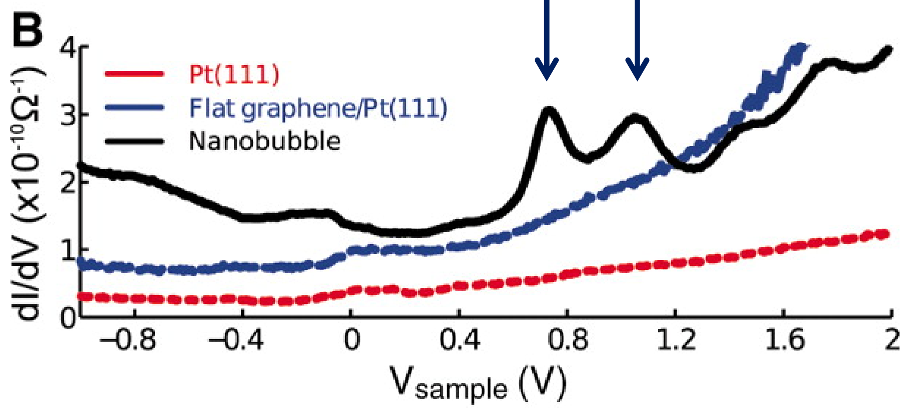

Levy, Burke, Meaker, Panlasigui, Zettl, Guinea, Castro Neto, Crommie - Science 329, 544 (2010)

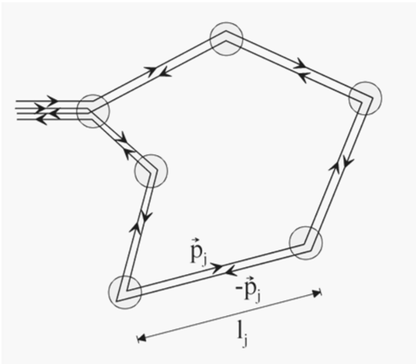

$$A^K_{\supset} \neq A^K_{\subset}$$

Inhomogeneous strain

$$\hat{H} = v\vec{\Sigma}\cdot\vec{p} + \hat{I}U(r) + \zeta\vec{\alpha}_{def}\cdot\vec{\Sigma}$$

Foster, Ludwig - PRB 73, 155104 (2006)
Morpurgo, Guinea - PRL 97, 196804 (2006)

$$\sigma = \sigma_{cl} \boxed{\cancel{+\frac{e^2}{2\pi h}\ln\left(\min[\tau_\varphi,\tau_B]/\tau\right)}}$$

Relaxation time τ_*

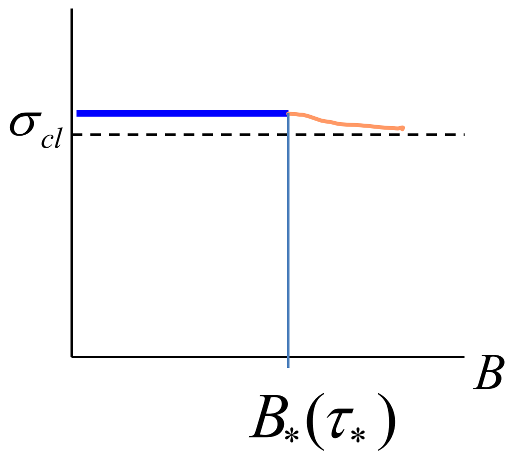

~~chiral electrons~~ $\cancel{\psi_{out} = e^{-i\phi(\Sigma_z/2)}\psi_{in}}$

$$\cancel{A_{\subset}A^*_{\supset} = e^{-i2\pi(\Sigma_z/2)}\,|A_{\subset}|^2 = -|A_{\subset}|^2 < 0}$$

... but strain has the opposite effect on electrons in K and K' valleys, so that the true time-reversal symmetry is preserved, and the inter-valley scattering restores the WL behaviour typical for electrons in time-inversion symmetric systems.

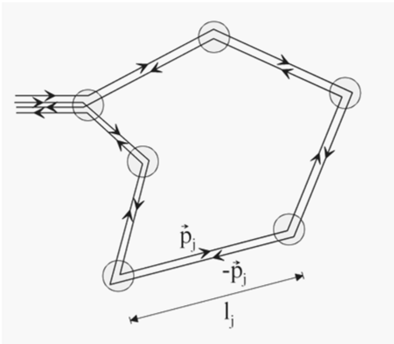

$$\boxed{A_{\supset}^{K_{\pm}} = A_{\subset}^{K_{\mp}}}$$

Intervalley time τ_{iv}

$$\boxed{\sigma = \sigma_{cl} - \frac{e^2}{2\pi h}\ln\left(\min[\tau_\varphi, \tau_B]/\tau_{iv}\right)}$$

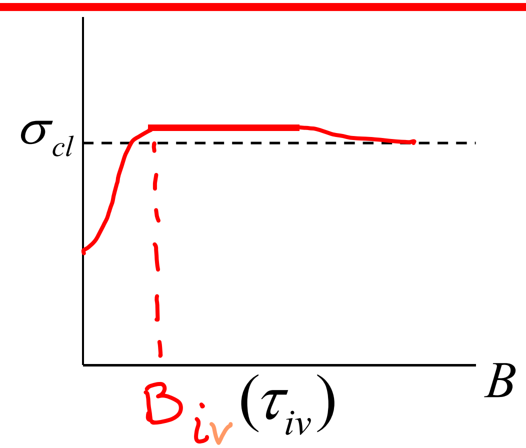

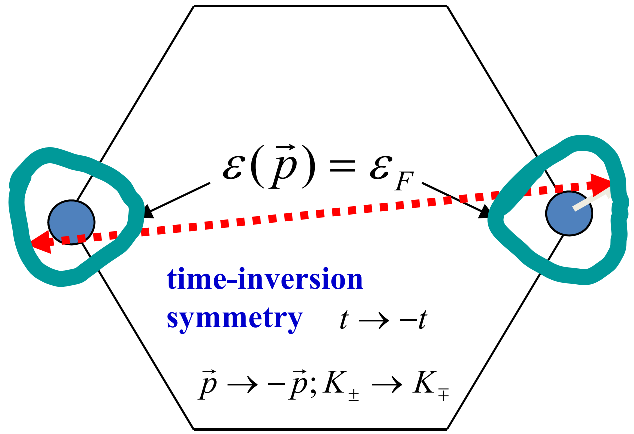

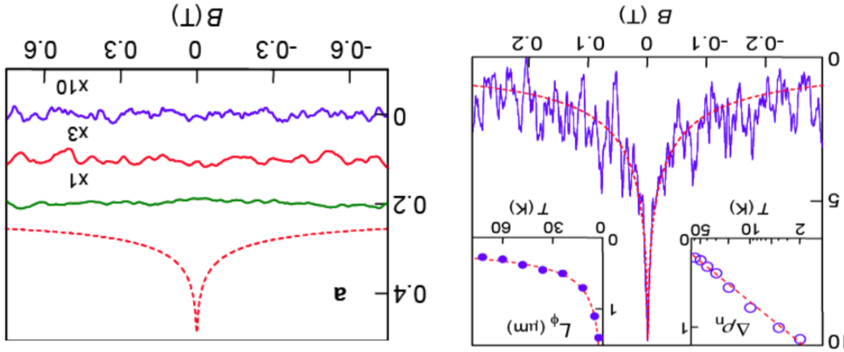

Morozov et al, PRL 97, 016801 (2006)

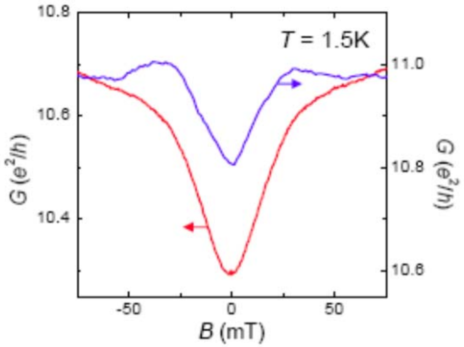

Heersche et al,
Nature 446, 56-59 (2007)

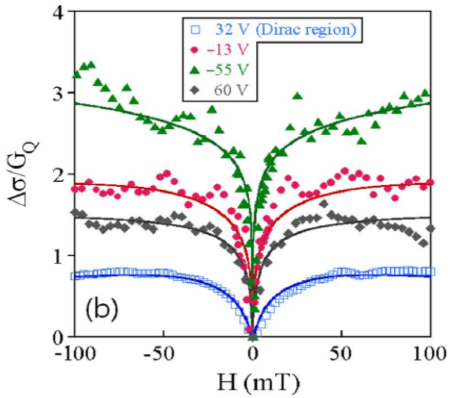

Ki et al,
PR B 78, 125409 (2008)

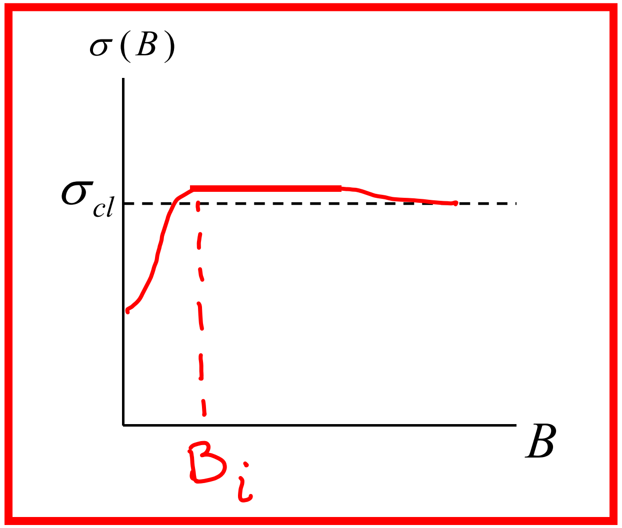

$$\tau_* << \tau_{iv} << \tau_\varphi$$

$$\tau_\varphi^{-1}(T) = \frac{T/\hbar}{\sigma h/e^2} \ln \frac{\sigma h}{2e^2}$$

$$B_{\varphi,*,iv} = \frac{\hbar/e}{4L_{\varphi,*,iv}} = \frac{\hbar/e}{4D\tau_{\varphi,*,iv}}$$

$$\Delta\sigma \sim \frac{e^2}{\pi h}\left(2F\left(\tfrac{B}{B_\varphi + B_* + B_{iv}}\right) + F\left(\tfrac{B}{B_\varphi + 2B_{iv}}\right) - F\left(\tfrac{B}{B_\varphi}\right)\right)$$

$$F(z) = \ln z + \psi\left(\tfrac{1}{2} + z^{-1}\right)$$

McCann, Kechedzhi, Fal'ko, Suzuura, Ando, Altshuler, PRL 97, 146805 (2006)

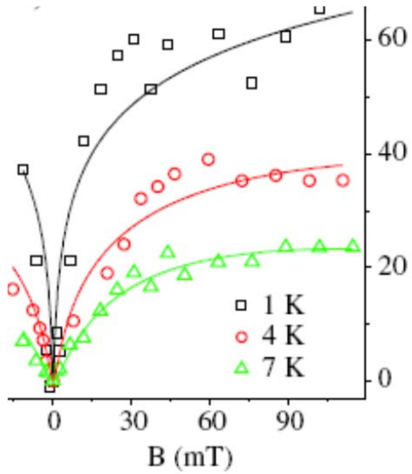

Tikhonenko *et al*
PRL 100, 056802 (2008)

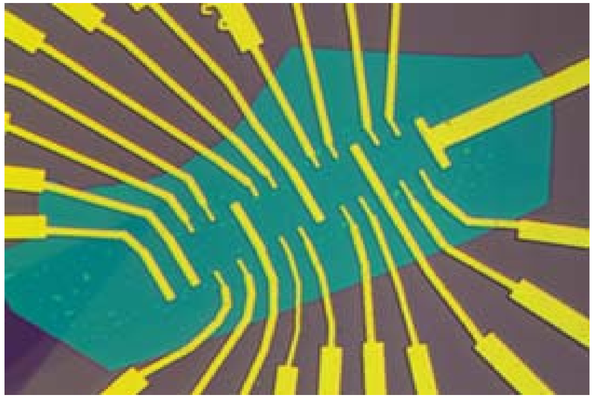

$$\tau_* \sim \tau$$

is an indication for that random strain fluctuations are the dominant source of disorder

data for graphene on SiO_2, $SrTiO_3$, hBN

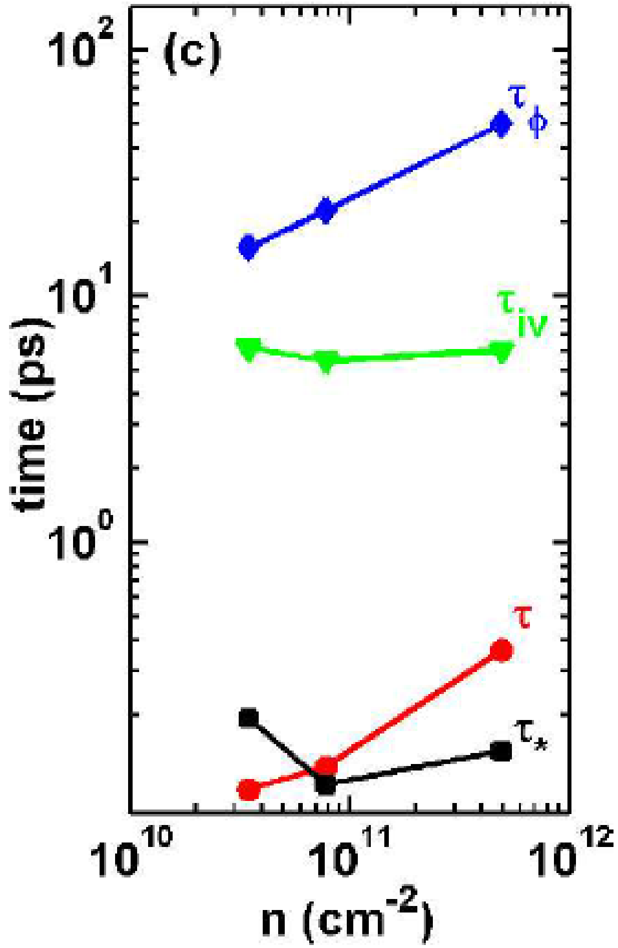

Couto, Costanzo, Engels, Ki, Watanabe, Taniguchi, Stampfer, Guinea, Morpurgo - PRX 4, 041019 (2014)

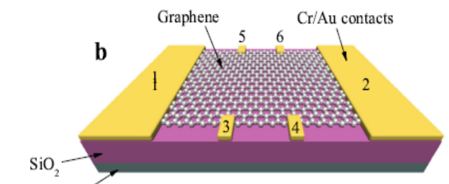

Sample	Size L×W	Mobility I	II	III
S1	41×18	13400	9800	7700

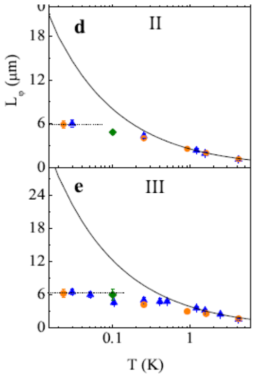

Kozikov, Horsell, McCann, Falko
Phys. Rev. B 86, 045436 (2012)

G/SiC

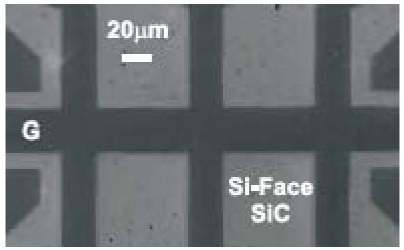

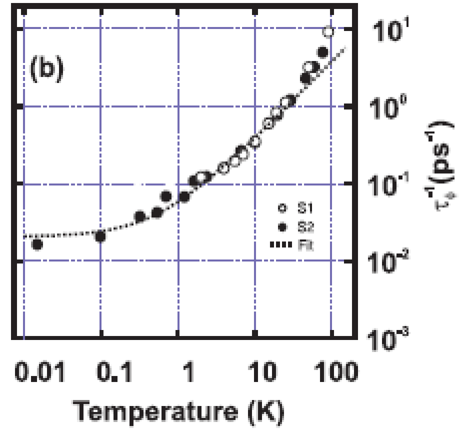

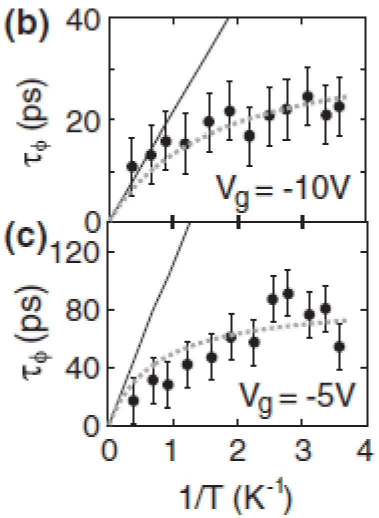

Saturation of decoherence time at low temperatures hints that there are spin-flip processes

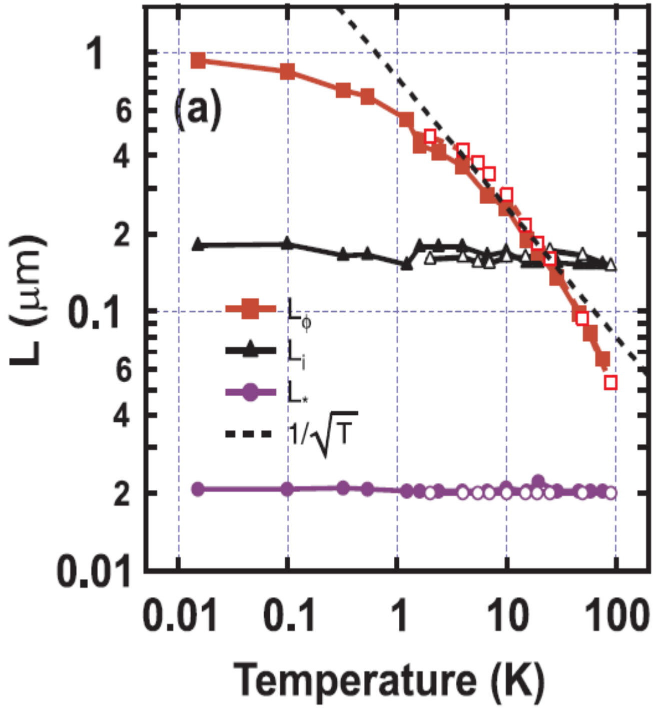

Engels, Terres, Epping, Khodkov, Watanabe, Taniguchi, Beschoten, Stampfer PRL 113, 126801 (2014)

Lara-Avila, Tzalenchuk, Kubatkin, Yakimova, Janssen, Cedergren, Bergsten, Falko – PRL 107, 166602 (2011)

WL in epitaxial graphene on SiC

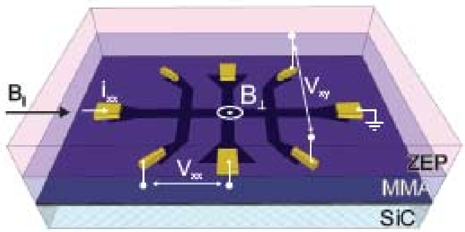

b)

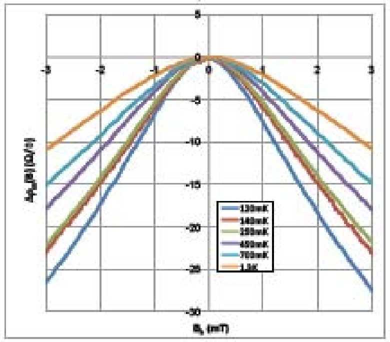

c)

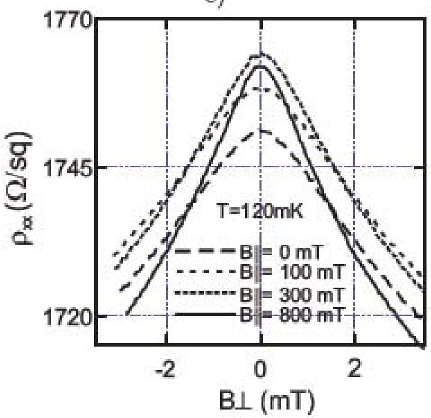

defect polarisation by in-plane magnetic field should restore a longer phase coherence time

$$\left.\frac{\partial^2 \sigma_{xx}}{\partial B_\perp^2}\right|_{B_\perp=0} = \frac{16\pi}{3}\frac{e^2}{h}\left(\frac{D\tau_\varphi}{h/e}\right)^2$$

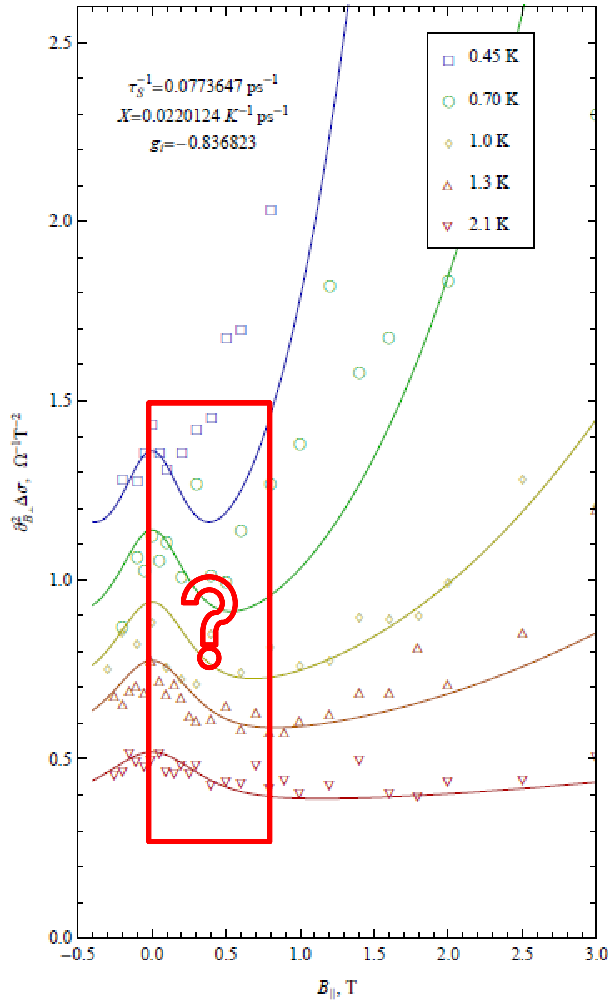

Lara-Avila, Kubatkin, Kashuba, Folk, Luscher, Yakimova, Janssen, Tzalenchuk, Fal'ko. PRL 115, 106602 (2015)

Influence of spin-flip scattering and scatter's spin dynamics on WL

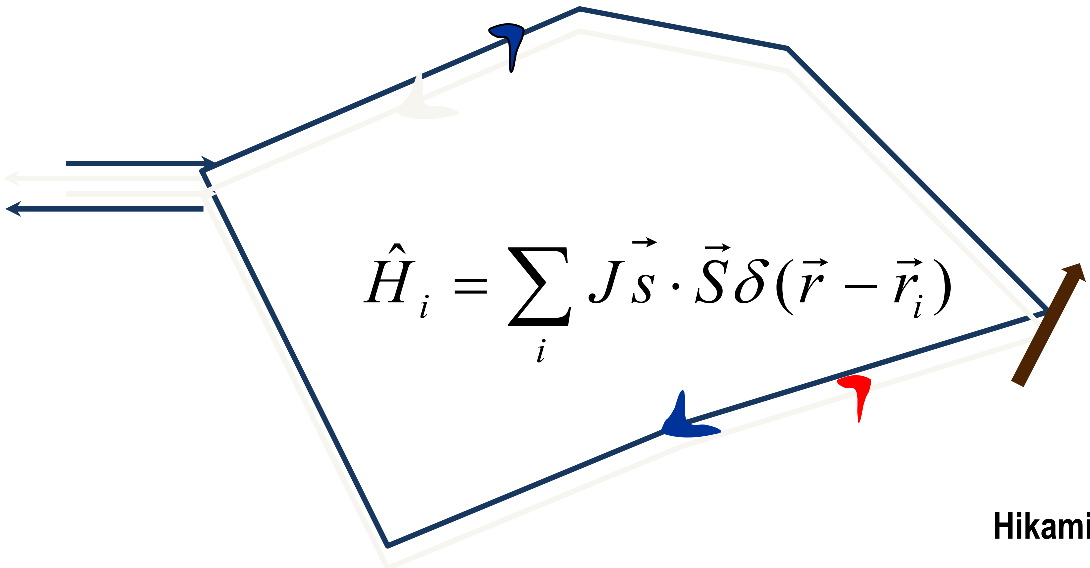

$$\hat{H}_i = \sum_i J\vec{s} \cdot \vec{S}\,\delta(\vec{r} - \vec{r}_i)$$

$$\tau_\varphi^{-1} \to \tau_\varphi^{-1} + \tau_s^{-1}$$

$$\tau_s^{-1} \propto n_i e^{-\mu_B g_i B/kT} J^2 S(S+1)$$

Hikami, Larkin, Nagaoka - Prog Theor Phys 63, 707 (1980)

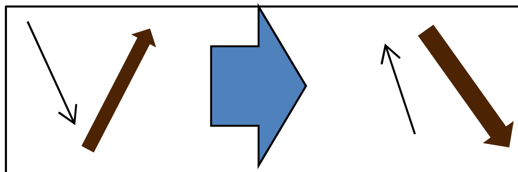

spin-flip in scattering, suppresses interference correction, in addition to spin relaxation

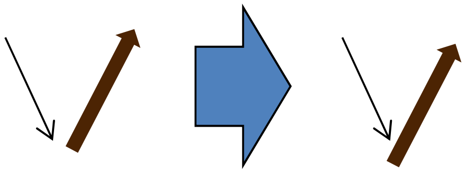

no-spin-flip:
this does not cause decoherence, but scattering amplitude/phase depend on the mutual orientation of defect's and arriving electron's spins

Influence of scatterer's spin dynamics on WL

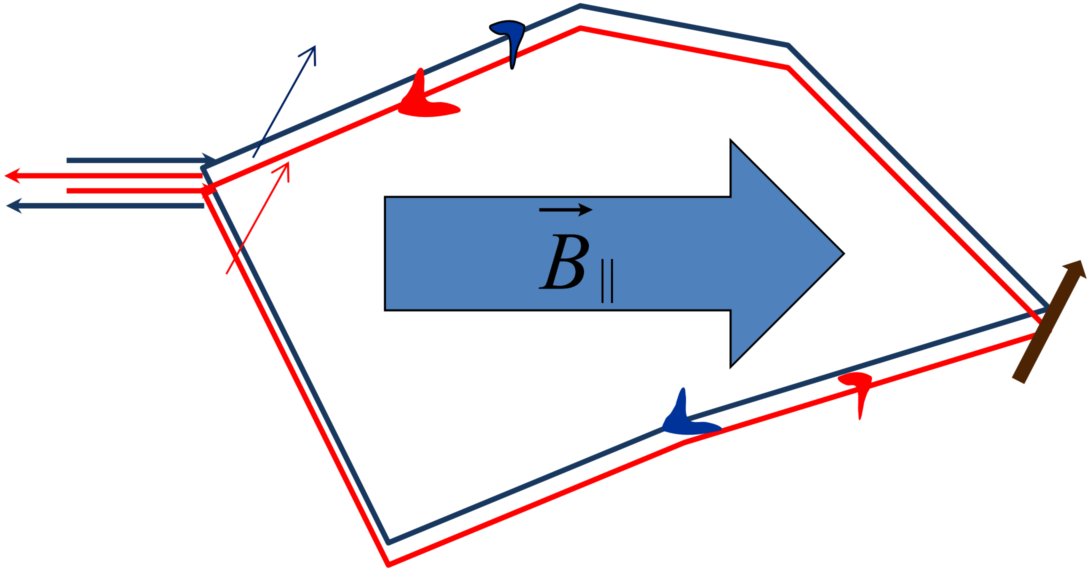

Difference of scattering conditions between clockwise and anti-clockwise trajectories, at

$$|t_{\supset} - t_{\subset}|(\omega_e - \omega_i) > 1$$

leads to faster de-coherence:

$$B_{\parallel} > \tau_s^{-1} / \mu_B |g_i - g_e|$$

$t = 0$

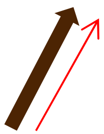

	$\omega_e = \omega_i$	$\omega_e \neq \omega_i$
$t = t_{\supset}$	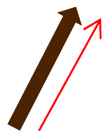	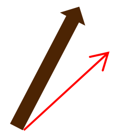
$t = t_{\subset}$	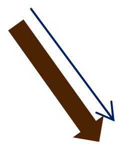	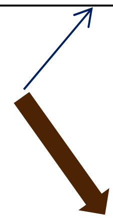

Kashuba, Glazman, Fal'ko - PRB 93, 045206 (2016)

Influence of scatterer's spin dynamics on WL

Lara-Avila, Kubatkin, Kashuba, Folk, Luscher, Yakimova, Janssen, Tzalenchuk, Fal'ko - PRL 115, 106602 (2015)

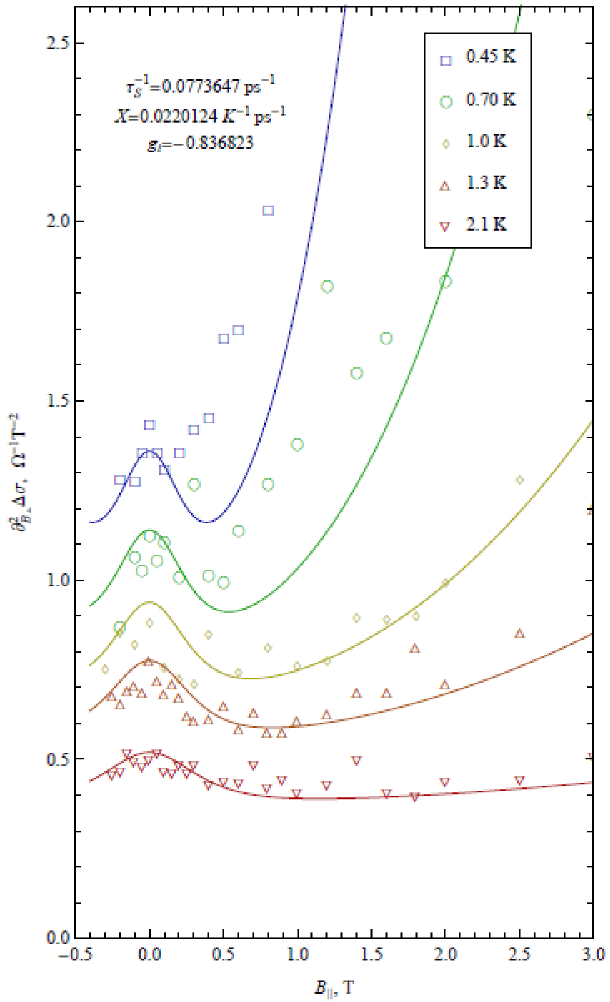

Kashuba, Glazman, Fal'ko - PRB 93, 045206 (2016)

For $g_i \neq g_e$ difference of scattering conditions between clockwise and anti-clockwise trajectories leads to a faster decoherence for

$$\frac{h\tau_s^{-1}}{\mu_B|g_i - g_e|} < B_{||} << \frac{kT}{\mu_B g_i}$$

$$\boxed{\begin{array}{l} g_e \approx 2 \\ g_i \approx -1 \end{array}}$$

Si substitutions of C in the dead carbon layer on SiC (Si has stronger SO coupling than carbon)

SO coupling and WAL/WL crossover in graphene

random potential

strain and sublattice asymmetry

inter-valley scattering

$$\hat{H} = v\vec{\Sigma}\cdot\vec{p} + \hat{I}\,u(\vec{r}) + \sum_{\alpha=x,y,z} u_{\alpha z}(\vec{r})\Sigma_\alpha\Lambda_z + \sum_{\substack{\alpha=x,y,z\\ l=x,y}} u_{\alpha l}(\vec{r})\Sigma_\alpha\Lambda_l$$

$z\to -z$ symmetric: conserves s_z but breaks time-inversion for the orbital motion of spin-up/down electrons.

$$+\ \Delta\Sigma_z s_z$$

$$+\sum_{l=x,y,z} a_{lz}(\vec{r})s_z\Lambda_l$$

$$+\ \alpha_{BR}\vec{\Sigma}\cdot(\vec{s}\times\vec{l}_z)$$

$$+\sum_{\substack{s=x,y\\ l=x,y,z}} a_{sl}(\vec{r})s_s\Lambda_l$$

$z\to -z$ asymmetric, relaxes all spin components

McCann, Fal'ko - PRL 108, 166606 (2012)

WAL due to proximity-induced SO coupling in graphene on transition metal dichalcogenides

$$\Delta\sigma(B) = -\frac{e^2}{\pi h}\left[F\left(\frac{\tau_B^{-1}}{\tau_\phi^{-1}}\right) - F\left(\frac{\tau_B^{-1}}{\tau_\phi^{-1} + 2\tau_{\text{asy}}^{-1}}\right) - 2F\left(\frac{\tau_B^{-1}}{\tau_\phi^{-1} + \tau_{\text{so}}^{-1}}\right)\right]$$

$$\tau_{iv}^{-1} >> \tau_{so}^{-1} \sim \sum_{l,s=all} |a_{l,s}|^2 + \left(\frac{\Delta}{\varepsilon_F}\right)^2 \tau^{-1} + 2\tau\,(\alpha_{BR}/\hbar)^2$$

Dyakonov-Perel relaxation

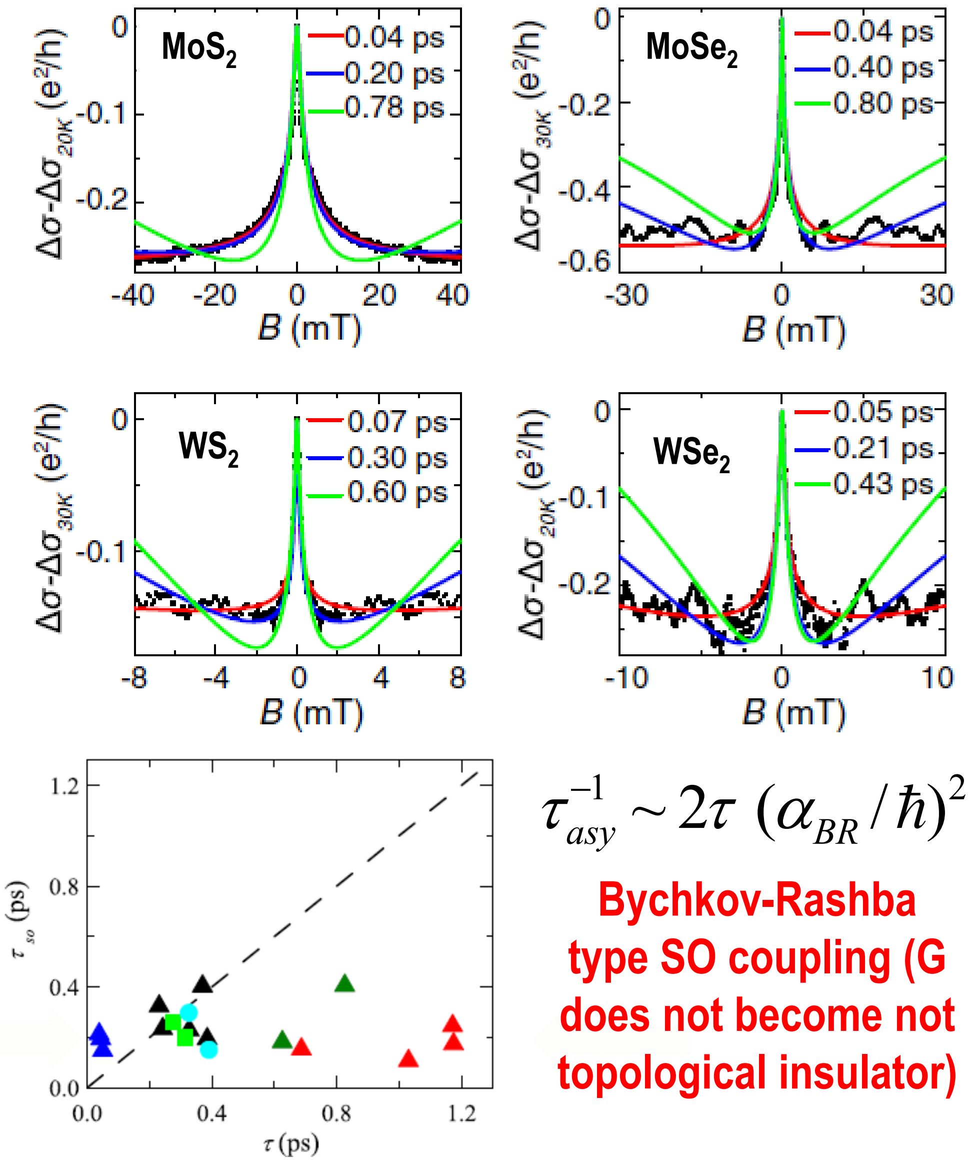

$$\tau_{asy}^{-1} \sim 2\tau\,(\alpha_{BR}/\hbar)^2$$

Bychkov-Rashba type SO coupling (G does not become not topological insulator)

McCann, Fal'ko - PRL 108, 166606 (2012); Wang, Ki, Khoo, Mauro, Berger, Levitov, Morpurgo - PRX 6, 041020 (2016)


✓ QHE in G and quantum resistance standard
✓ weak localisation regimes in disordered graphene
Ed McCann (Lancaster)
Sergey Kopylov (kopylov.com ltd)
Sergey Slizovskiy (NGI)
Oleksiy Kashuba (Wurzburg)
Leonid Glazman (Yale)
Boris Altshuler (Columbia)
Alexander Tzalenchuk (NPL)
JT Janssen (NPL)
Sergey Kubatkin (Chalmers)
Joshua Folk (Vancouver)
Rositsa Yakimova (Linkoping)
Ziad Melhem (Oxford Instruments)
EPSRC
erc
GRAPHENE FLAGSHIP

Quantum transport in graphene

L1 Disordered graphene (G)

graphene 101

QHE in G and quantum resistance standard

weak localisation regimes in graphene

L2 Ballistic electrons in graphene

L3 Moiré superlattice effects in G/hBN heterostructures

Influence of bilayer inclusions

Bilayer inclusions in a monolayer matrix formed on the step edges

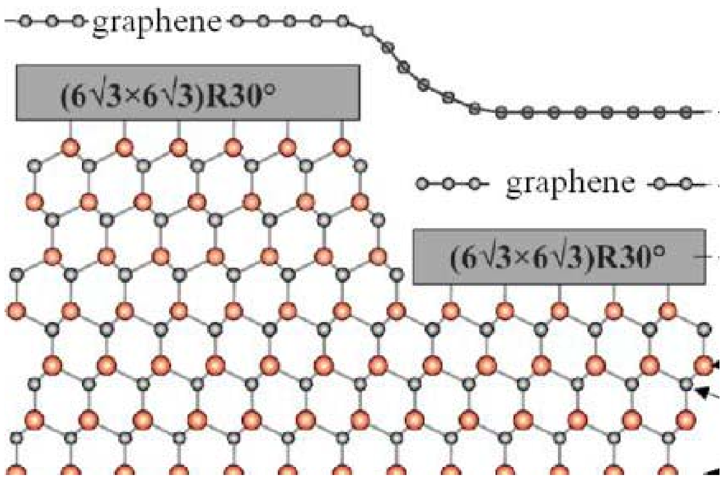

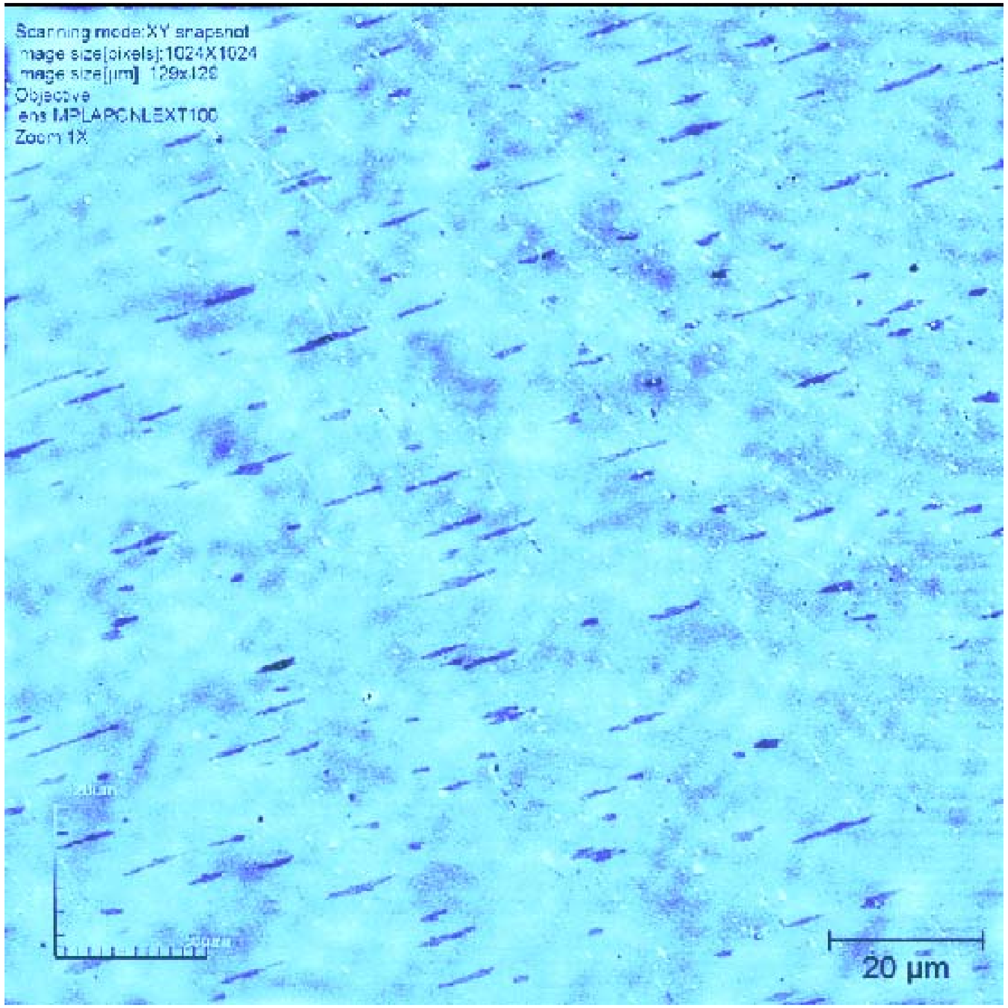

T. Yager *et al., Nano Lett.* **13**, 4217–4223 (2013)

Influence of bilayer inclusions

Interlayer asymmetry gap opened by the transverse electric field

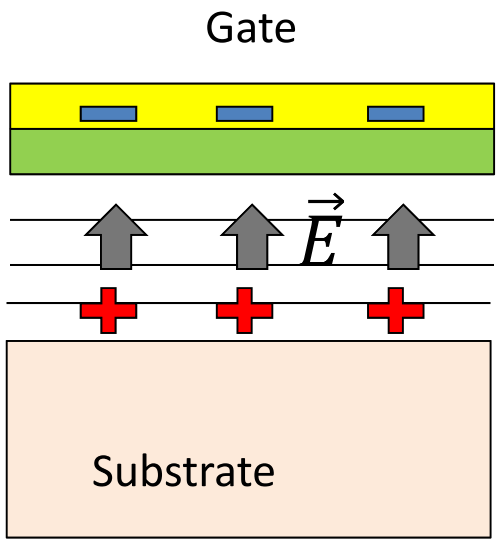

Metallic bilayer

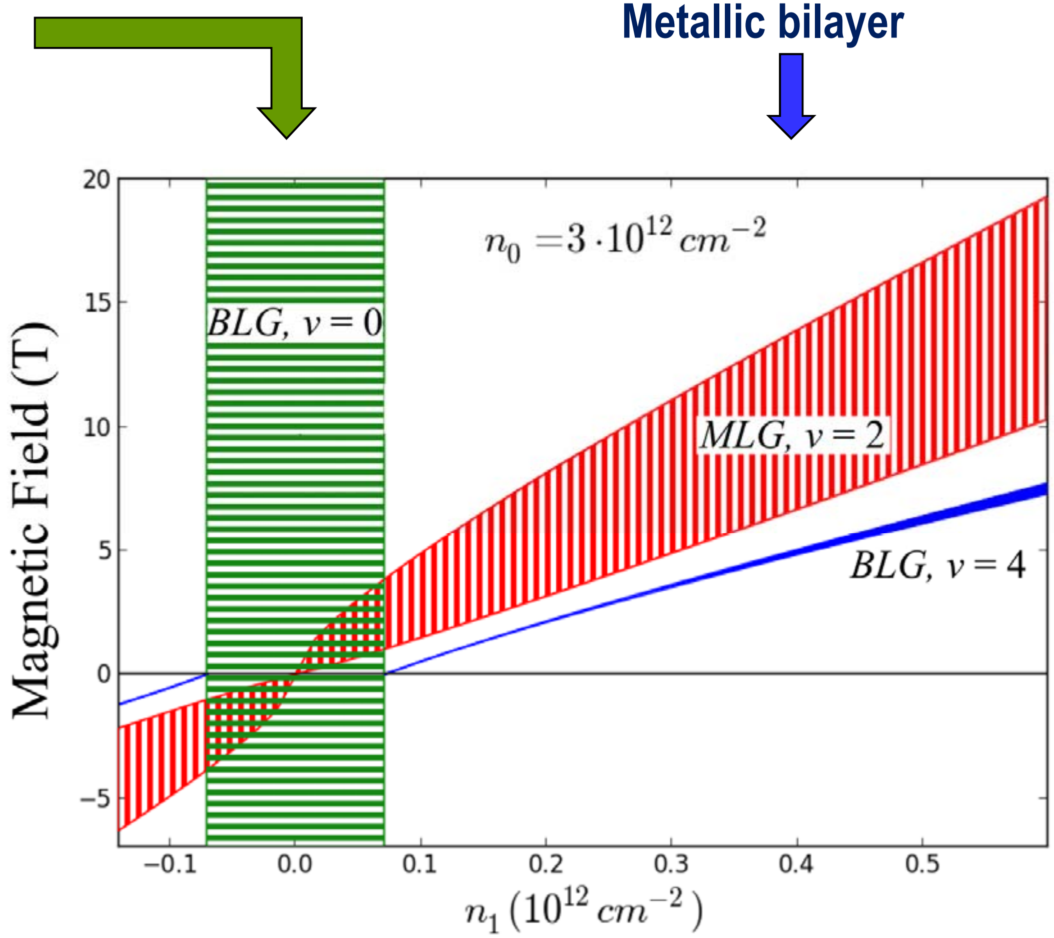

Chua, Connolly, Lartsev, Yager, Lara-Avila, Kubatkin, Kopylov, Fal'ko, Yakimova, Pearce, Janssen, Tzalenchuk, Smith - Nano Letters, 14, 3369 (2014)

Influence of bilayer inclusions

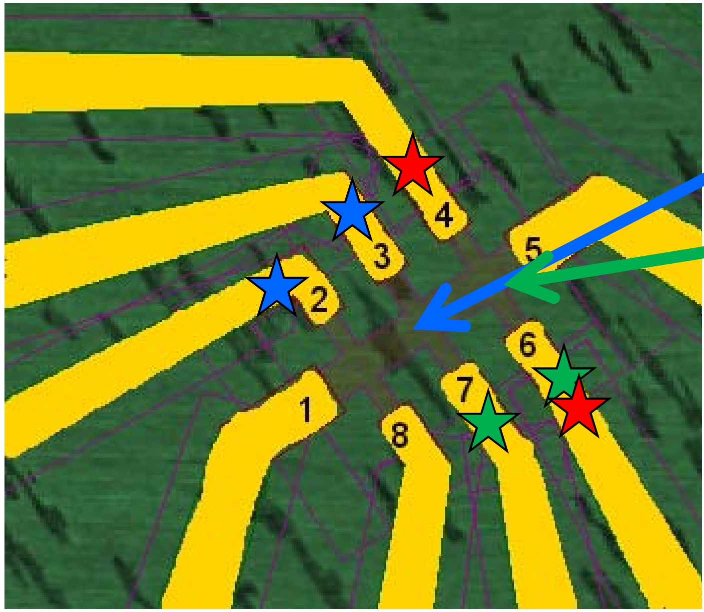

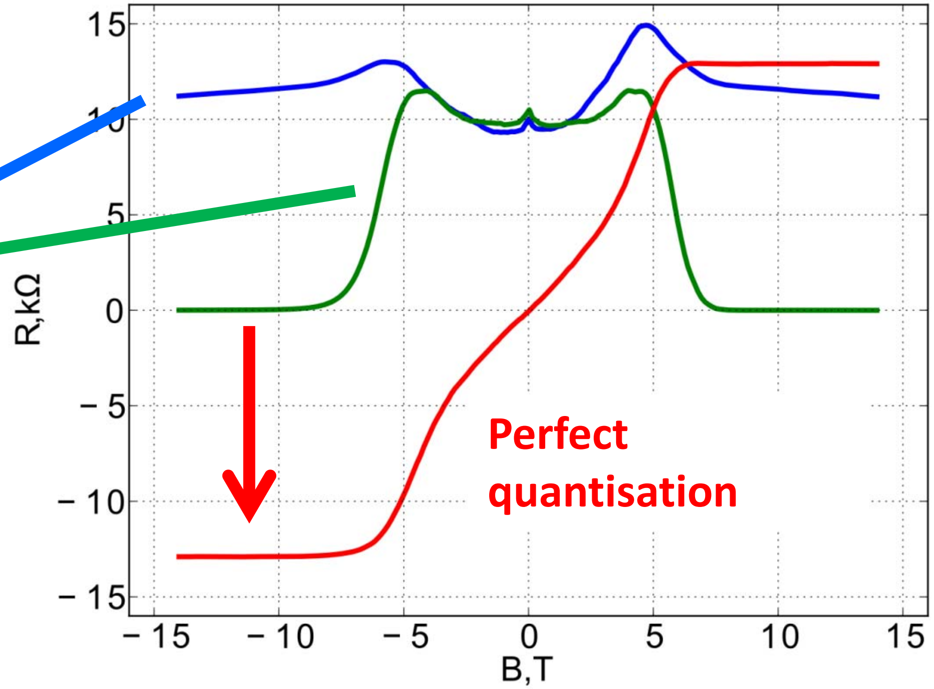

Bilayer inclusions act as metallic shunts

Chua, Connolly, Lartsev, Yager, Lara-Avila, Kubatkin, Kopylov, Fal'ko,
Yakimova, Pearce, Janssen, Tzalenchuk, Smith - Nano Letters, 14, 3369 (2014)

Influence of bilayer inclusions

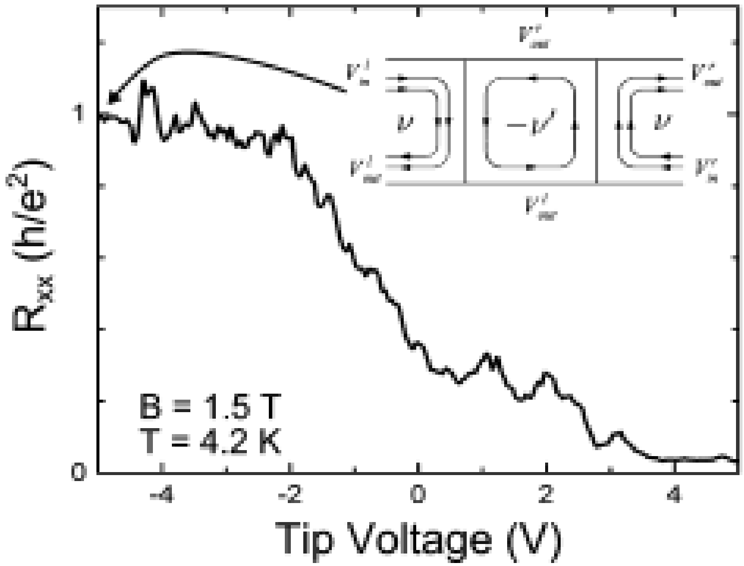

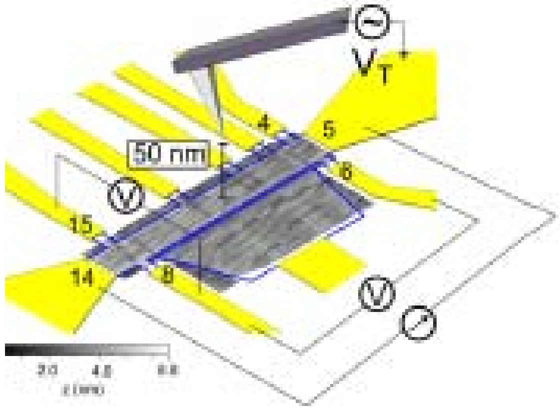

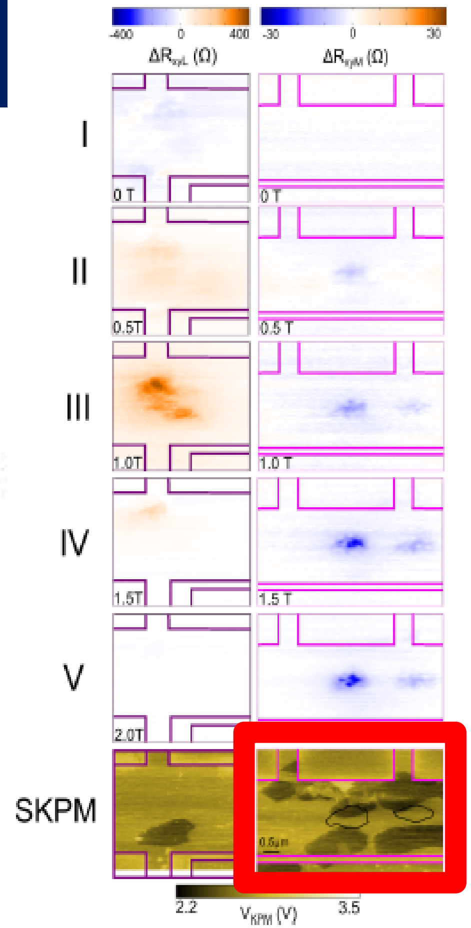

$$R_{6\text{-}8} \equiv \frac{(V_{\text{out}}^{\text{l}} - V_{\text{in}}^{\text{r}})}{I} = \frac{\nu + \nu'}{\nu\nu'}\frac{h}{e^2} \xrightarrow[\nu=\nu'=2]{} \frac{h}{e^2}$$

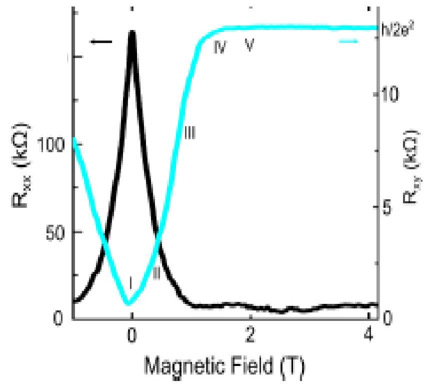

Chua, Connolly, Lartsev, Yager, Lara-Avila, Kubatkin, Kopylov, Fal'ko, Yakimova, Pearce, Janssen, Tzalenchuk, Smith - Nano Letters, 14, 3369 (2014)